Downloaded from orbit.dtu.dk on: Jul 09, 2018

Technical University of Denmark

A methodology for designing flexible multi-generation systems

Lythcke-Jørgensen, Christoffer Ernst; Viana Ensinas, Adriano; Münster, Marie; Haglind, Fredrik

Published in:
Energy

Link to article, DOI:
10.1016/j.energy.2016.01.084

Publication date:
2016

Document Version
Peer reviewed version

Link back to DTU Orbit

Citation (APA):
Lythcke-Jørgensen, C. E., Viana Ensinas, A., Münster, M., & Haglind, F. (2016). A methodology for designing flexible multi-generation systems. Energy, 110, 34–54. DOI: 10.1016/j.energy.2016.01.084

DTU Library
Technical Information Center of Denmark

General rights
Copyright and moral rights for the publications made accessible in the public portal are retained by the authors and/or other copyright owners and it is a condition of accessing publications that users recognise and abide by the legal requirements associated with these rights.

- Users may download and print one copy of any publication from the public portal for the purpose of private study or research.
- You may not further distribute the material or use it for any profit-making activity or commercial gain
- You may freely distribute the URL identifying the publication in the public portal

If you believe that this document breaches copyright please contact us providing details, and we will remove access to the work immediately and investigate your claim.

*Manuscript
Click here to download Manuscript: Manuscript 2.1..docx Click here to view linked References

A methodology for designing flexible multi-generation systems

Christoffer Lythcke-Jørgensen [a]*, Adriano Viana Ensinas [b], Marie Münster [c], Fredrik Haglind [a].

[a] Technical University of Denmark, Mechanical Engineering

[b] École Polytechnique Fédérale de Lausanne, Industrial Process and Energy Systems Engineering

[c] Technical University of Denmark, Management Engineering

* Corresponding author. Email: celjo@mek.dtu.dk. Phone: +45 30 42 72 00. Nils Koppels Allé 403, 2800 Kgs. Lyngby, Denmark.

Abstract

A flexible multi-generation system (FMG) consists of integrated and flexibly operated facilities that provide multiple links between the various layers of the energy system. FMGs may facilitate integration and balancing of fluctuating renewable energy sources in the energy system in a cost- and energy-efficient way, thereby playing an important part in smart energy systems.

The development of efficient FMGs requires systematic optimization approaches. This study presents a novel, generic methodology for designing FMGs that facilitates quick and reliable pre-feasibility analyses. The methodology is based on consideration of the following points: Selection, location and dimensioning of processes; systematic heat and mass integration; flexible operation optimization with respect to both short-term market fluctuations and long-term energy system development; global sensitivity and uncertainty analysis; biomass supply chains; variable part-load performance; and multi-objective optimization considering economic and environmental performance.

Tested in a case study, the methodology is proved effective in screening the solution space for efficient FMG designs, in assessing the importance of parameter uncertainties and in estimating the likely performance variability for promising designs. The results of the case study emphasize the importance of considering systematic process integration when developing smart energy systems.

Keywords: Design optimization, energy efficiency, flexible operation, multi-generation, polygeneration, smart energy systems

Nomenclature

Latin letters

A_a	Area size	[km^2]
b	Number of parameter value levels in Morris screening	[-]
C_{HEN}	Heat exchanger network investment cost	[Euro]
$C_{inv,k}$	Process investment cost	[Euro]
$C_{inv,k0}$	Process reference investment cost	[Euro]
c_b	Marginal biomass cost	[Euro]
c_{b0}	Reference biomass cost	[Euro]
$c_{b,tr}$	Marginal biomass logistics cost	[Euro]
c_{op}	Operating cost	[Euro]
D_p	Uncertainty distribution of parameter p	[-]
$d_{tr,a}$	Mean transportation distance from area a	[km]
$\dot{e}_f$	Thermal energy flow	[kW]
EE	Elementary effect	[-]
f	Model output function	
G_i	CHOP group	
$\Delta H_{s,i}$	Sum of enthalpy flows in temperature interval s	[kW]

45	i	Annual discount rate	[-]
46	M	Number of uncertain model parameters	[-]
47	M_f	Investment scaling constant	[-]
48	$\dot{m}_f$	Mass flow	[kg/s]
49	$mean_i$	Estimated standard error of the mean	[-]
50	$N_{CHOP,max}$	Maximum number of CHOP groups	[-]
51	n_p	Number of characteristic parameter intervals	[-]
52	O_j	Operating point	
53	p	Parameter	
54	q_a	Annual biomass cultivation in area a	[ton]
55	$q_{b,an}$	Annual biomass demand	[ton]
56	R	Product or service market	
57	R_{th}	Thermal energy market	
58	R_b	Local biomass market	
59	r_a	Maximum transportation distance, area a	[km]
60	s_{max}	Number of temperature intervals	[-]
61	T	Temperature	[°C]
62	t_i	CHOP group, duration	[h]
63	t_j	Operating point, duration	[h]
64	$t_{PV,i}$	CHOP group, present value factor	[h]
65	w	Number of repetitions in Morris screening	[-]
66	Y_j	Operating point, year of occurrence	[-]
67	y_k	Installation delay of process k	[years]
68	y_{lt}	Facility lifetime	[years]
69	Z_0	Global warming potential	[tCO_2]

z_{inv}	Global warming potential of investments	[tCO_2]
z_{op}	Global warming potential of operation	[tCO_2]

Greek letters

Δ	Perturbation factor in Morris screening	[-]
$\lambda_{k,i}$	Process load of process k in period i	[-]
$v_{k,i}$	Operation of process k in period i	[-]
σ_k	Dimension of process k	[-]
σ_{k0}	Process k reference dimension	[-]
σ_{ut}	Utility process dimension	[-]
ω_k	Installation decision for process k	[-]

Subscripts

a	Biomass cultivation area index
b	Biomass flow index
f	Thermal and mass flow index
i	Period index
j	Operating point index
k	Process index
l	Layer index, used in the Mixed Integer-Linear Programming model
n	Characteristic parameter interval index
p	Parameter index
r	Market index
s	Temperature interval index
0	Reference

Abbreviations

94	AD	Combined anaerobic digester and biogas upgrading facility
95	BB	Biomass boiler
96	CCHP	Combined cooling, heating and power
97	CHOP	Characteristic operating pattern
98	CHP	Combined heat and power
99	DESS	Distributed energy supply system
100	FMG	Flexible multi-generation system
101	GB	Gas boiler
102	GT	Gas turbine
103	GWP100a	100-years global warming potential
104	HP	Ground-based district heating heat pump
105	LCA	Life cycle assessment
106	MILP	Mixed integer-linear programming
107	MINLP	Mixed integer-nonlinear programming
108	NPV	Net present value
109	SMG	Static multi-generation plant
110	SR	Steam Rankine cycle

111

1. Introduction

Flexible multi-generation systems (FMGs) are integrated, dynamic facilities that convert one or several energy resources into multiple energy services and other valuable products, e.g. electricity, heating, cooling, bio-fuels, and bio-chemicals [1]. FMGs are characterised by their ability to adjust operation in response to fluctuating demand patterns and varying price schemes. In the present work, the following definition of an FMG is introduced:

- A flexible multi-generation system (FMG) is a system of integrated facilities that provide multiple links between layers of the energy system, enabling adjustable operation in response to changes in prices and demands of the consumed and delivered services.[1]

The main advantages of FMGs are: The embedded possibility for optimizing operation by altering feedstock, products and services depending on demand and market price [2][3][4]; the possibility of integrating and balancing generation from intermittent renewable energy resources such as wind, solar, wave and tidal in a cost-efficient way [5][6][7], and the possibility of achieving high aggregated conversion efficiencies through process integration [8][9][10][11]. Through the conversion, conditioning and storing of multiple energy vectors, FMGs integrate the various layers of the energy system and are capable of providing supply-demand flexibility that can counteract energy system imbalances induced by e.g. intermittent renewable energy sources. In principle, FMGs can therefore be seen as efficient energy system valves that may play an important part in the development and operation of smart energy systems [12][13]. The generic FMG concept is illustrated in Figure 1.

[1] In specific cases, the definition of an FMG may be overlapping with the terms 'polygeneration' and 'energy hubs'. In a recent review, Adams and Ghouse [75] have defined 'polygeneration' as a thermochemical process which simultaneously generates electricity and produces at least one type of chemical or fuel without being a co- or tri-generation unit. 'Energy hubs' may refer to homes, large energy consumers, power plants or regions [76] as well as integrated facilities [4][77]. The FMG definition is introduced here in order to characterize integrated facilities that may actively contribute to the balancing of the energy system.

By definition, FMGs may be either centralized facilities or distributed systems, as long as the various facilities are integrated. The present manuscript differentiates between a *plant,* in which all considered facilities are co-located, and a *system,* in which facilities are distributed on several locations. It should be emphasized that FMGs may include static processes, e.g. cellulosic ethanol production [14] as well as intermittent processes that are not fully dispatchable, e.g. wind turbines and solar heating, as long as the combined system has a degree of operational flexibility.

The issues to be considered when designing FMGs comprise: The selection of processes and technologies from many alternatives; geographical location, dimensioning, and integration of processes with respect to thermal and mass flows; operation optimization with respect to hourly demand and price fluctuations and long-term energy system development; determination of local resource availability; investment planning; systematic evaluation of design uncertainties; and consideration of both economic and environmental objectives. All of these issues must be considered simultaneously as they affect one another. To cope with this complexity, a systematic optimization approach is needed for the design of FMGs [8].

One branch of multi-generation plants treated in the literature combines the generation of power and production of chemicals. Gassner and Maréchal [15] presented a combined mixed integer-nonlinear programming (MINLP)/mixed integer-linear programming (MILP) methodology for the synthesis of facilities producing fuel from biomass through thermochemical conversion. The methodology considered the selection and dimensioning of processes, systematic process integration using pinch analysis, and assessment of multiple objectives including thermo-economic performance. In a second work the methodology was enhanced to allow for the systematic inclusion of life cycle assessment (LCA) in the design evaluation [16]. The methodology was later applied in a case study of a static multi-generation plant (SMG) generating fuel and electricity from biomass [17]. The developed methodology did not consider flexible operation and input parameter uncertainties.

Liu et al. studied SMGs generating power and methanol. In five related works, the group first presented a multi-period MILP model for the design and investment planning optimization of such SMGs whilst

156 considering static operating conditions over periods of 5 years [18]. The model was later upgraded to an
157 MINLP model [19] and extended to allow for multi-objective optimization [20] and stochastic programming
158 using a decomposition strategy [21]. The group further presented one methodology for general investment
159 planning and one for detailed design configuration of SMGs [22]. However, neither of the presented
160 methodologies considered short-term operation flexibility.
161 Chen et al. also studied the multi-generation of power and chemicals. In three consecutive works, the
162 group first presented a deterministic superstructure-based optimization model for designing static SMGs
163 coproducing power, naphtha, diesel, and methanol from coal and biomass [23]. The model was later
164 enhanced to allow for flexible operation optimization with respect to price variations over seasonal peak-
165 and off-peak periods, and, based on a case study, the group concluded that FMGs may achieve higher net
166 present values (NPVs) than static ones because of the operation flexibility, however at the cost of larger
167 investments [24]. In a third study, the group implemented a modified decomposition algorithm based on
168 the generalized Benders decomposition in their optimization model to reduce computational time [25], and
169 demonstrated in two case studies that the modified methodology achieved faster calculation times than
170 the BARON solver [26]. The group applied simple energy balances rather than detailed process integration
171 methodologies to simulate process integration possibilities, which may have led to overestimated efficiency
172 improvements, as also discussed by the authors [27]. Furthermore, uncertainties were not considered.
173 Another branch of multi-generation plants are facilities based on the combined generation of cooling,
174 heating, and power (CCHP), also known as trigeneration. Marnay et al. [28] presented a methodology for
175 minimizing the overall costs of CCHPs in commercial buildings by selecting and dimensioning technologies
176 and optimizing operation based on diurnal load profiles. Rubio-Maya et al. [29][30] presented a heuristic,
177 two-level approach for designing local FMGs generating power, heat, cooling and fresh water. Selection of
178 technologies and a preliminary process dimensioning were handled in a first step based on monthly-
179 averaged requirements, while a second step dealt with the final dimensioning of components, including
180 thermal energy storage, based on monthly mean-day demands. Piacentino et al. [31] presented a

deterministic MILP-based tool for optimizing trigeneration-based micro-grids with thermal storages with respect to NPV. Capuder and Mancarella [32][33] presented a framework for the techno-economic and environmental comparison of seven distributed FMG options for co-generating heat and power. The framework considered half-hour time steps on typical seasonal days, thermal energy storage, and ramp rate constraints between successive time periods. The group found that increased operation flexibility resulted in significant savings in investment and operating costs as well as in a reduced environmental impact when compared to the reference case of a district heating boiler. Recently, Capuder et al. [34] extended their work to consider the economic value of operational flexibility and investment flexibility under long-term operational uncertainty and found that consideration of investment flexibility both reduced expected costs and economic risks associated with investments in distributed FMGs co-generating heat and power.

With regard to distributed energy supply systems (DESS), Voll et al. [35] developed an approach for the superstructure-free synthesis and optimization of DESS using an evolutionary algorithm and applied the method on a numerical example of a DESS with time-varying heating and cooling loads. Following this, Voll et al. [36] presented a framework for automated superstructure generation and optimization of DESS using an MILP model. The group further developed a method for reducing non-linear DESS optimization problems into MILP models using a multivariate piecewise-affine surrogate modelling approach [37], and a method for exploring the near-optimal solution space when optimizing DESS [38]. In a recent study, the group presented a hybrid approach for optimizing the synthesis of renewable electricity systems by combining heuristic-based pre-selection of candidate technologies with the previously developed automated superstructure generation and optimization of DESS [39]. Zhou et al. [40] presented a two-stage stochastic programming model for designing DESS which further allowed for the consideration of uncertainties in the optimization. Finally, Leung Pah Han et al. [41] presented an iterative method combining MILP/MINLP for designing local production systems that integrate food, water, and energy systems based on annual demands, with the aim of minimizing the cumulative exergy destruction.

Concerning urban multi-generation plants, Lythcke-Jørgensen and Haglind [42] studied the design and operation optimization of an FMG generating power and heat and producing cellulosic ethanol. The study found that short-term operating patterns may be critical for the overall economy of FMGs. Maréchal et al. [43] presented a multi-period, multi-objective MINLP/MILP approach for deterministic design optimization that comprised technology selection and dimensioning, process integration, facility location selection, and network layout. By considering monthly static operating patterns, Fazlollahi and Maréchal [44] used parts of this methodology for designing FMGs that provide energy services for district energy systems. In three parallel works, the group extended their work by incorporating the following methodology: A method for approximating energy system conditions by a number of typical periods with hourly and aggregated multi-hour time steps [45]; a model of daily thermal storages [46]; and a model of distribution networks [47]. Shortcomings of the combined methodology are the facts that only cyclic short-term operating patterns may be considered using the typical periods approach, and that input parameter uncertainties are not considered.

This study presents a novel, systematic methodology for designing FMGs. It applies node-based superstructure representation and is based on a genetic algorithm and multi-period MILP approach [48]. The purpose of the methodology is to conduct quick and reliable pre-feasibility analyses of FMGs for assessing which of the facility designs that would be efficient in a given energy system context, rather than estimating the optimal performance of pre-defined facility designs. The novelty of the methodology lies in the fact that it simultaneously considers the following: Selection, location, and dimensioning of processes from many alternatives; systematic heat and mass integration using pinch analysis; flexible operation optimization with respect to both short-term market fluctuations and long-term energy system development through the application of the Characteristic Operating Pattern (CHOP) method [49]; investment planning; global sensitivity and uncertainty analysis; consideration of local resource availability, biomass supply chains, and market sizes; variable part-load performance; and multi-objective optimization

considering NPV and 100-years global warming potential (GWP100a). To the author's best knowledge, no previous methodology has considered all of these aspects in an integrated, systematic manner.

The paper is structured as follows: After the introduction, which also features a short literature review on methodologies for designing multi-generation systems, the developed design methodology is presented in Section 2. In Section 3, the methodology is applied in a case study of a conceptual FMG co-generating power and heat and producing cellulosic ethanol, synthetic natural gas, and fertilizer from natural gas, domestic and industrial waste, straw, and manure. Section 4 contains a discussion on advantages, drawbacks, and development possibilities for the design methodology. A conclusion on the study is given in Section 5.

2. Design methodology

The design methodology developed in the present study is a tool for optimizing the design and operation of FMGs by coupling process models with energy system information, as illustrated in Figure 2. The structure of the design methodology is presented in Figure 3, which illustrates how the optimization problem has been decomposed into several parts. The design methodology is introduced in this section, which is structured according to the five overarching steps of the methodology.

2.1. Input data

In general, four types of input data are required for running the design methodology: Process and equipment models, energy system data, local resource data, and life cycle inventory data. If sensitivity and uncertainty analyses are to be performed on selected designs, uncertainty distributions for input data D_p must be defined for all the considered uncertain input parameters p.

Process and equipment models

The first input to the design methodology is models of the processes and equipment to be considered for the FMG. The models can be detailed thermodynamic and chemical models as well as simpler black box

253 models, as long as they provide the information required for developing surrogate models, as discussed in
254 Section 2.2.

255 **Energy system data**

256 The second input to the design methodology is data on the surrounding energy system that the FMG is to
257 operate within. Depending on the processes considered, energy system data may include parameters such
258 as power price, demands for district energy, fossil fuel prices, subsidy schemes etc. All information must be
259 provided for short time intervals, a few hours or less, in order to include details on short-term fluctuations
260 in prices and demands that the FMG may respond to. The data must be provided for the entire lifetime of
261 the FMG.

262 **Local resource data**

263 Local resource data describe the availability, costs, and logistics of local resources considered for processing
264 in the FMG, e.g. biomass, manure, domestic, and industrial waste etc. This information can be essential for
265 the economic viability of FMGs, as transportation and storage costs for processing locally distributed
266 resources may induce a diseconomy-of-scale trend that can exceed the economy-of-scale benefits for
267 larger processing equipment, as also discussed by Jack [50].

268 **Life cycle inventory data**

269 The environmental impact parameter considered in the design methodology is the 100-years global
270 warming potential (GWP100a). GWP100a is an indicator of the global warming impact over a 100-year
271 period from materials mining, production of equipment, installation, operation and maintenance, and
272 decommissioning of a facility, measured in equivalent tons of CO_2 emissions. In order to consider the
273 minimization of GWP100a when designing FMGs, life cycle inventory data must be provided on all
274 considered process equipment, consumed resources, displaced production and consumption etc.

2.2. Structuring phase

2.2.1. CHOP-reduction of external operating conditions

In order to reduce computation time, external operating conditions are reduced using the Characteristic Operating Pattern (CHOP) method introduced by Lythcke-Jørgensen et al. [49]. The CHOP method is a visually-based aggregation method for clustering data on external operating conditions. Aggregation is conducted based on important parameter values rather than time of occurrence, thereby preserving important information on short-term relations between the relevant operating parameters. The CHOP method is briefly introduced below. Details on contents, validation, and application of the CHOP method have been given previously [49].

The CHOP method assumes quasi-static operation and is applicable on datasets in the form of operating points O_j, with each point being characterised by a year of occurrence after operation initiation Y_j, a duration t_j, and a number of operating condition parameters $\boldsymbol{p_j}$.

$$O_j = \{Y_j, t_j, \boldsymbol{p_j}\} \quad (1)$$

A principal sketch of the data aggregation principle applied in the CHOP method is presented in Figure 4.

The CHOP method consists of the three principal steps, which are described below:

1: Entity selection

In the first step of the CHOP-method, the user has to identify the relevant volatile operating parameters $\boldsymbol{p}$ for the FMG of interest. The parameters selected are to be seen as boundary conditions for the operation of the FMG, and parameter values are therefore assumed to be unaffected by FMG operation. This assumption needs to be validated, perhaps à posteriori, when applying the design methodology. Relevant operating parameters could be power price, fossil fuel prices, and CO_2 tax schemes, depending on the processes considered for the FMG and the energy system of interest. If price functions can be established for some boundary conditions as a function of FMG operation, the function constants can be captured in the vector $\boldsymbol{p_i}$ as well.

2: Clustering criteria

Having identified the relevant parameters $\boldsymbol{p}$, the second step is to define the criteria for clustering operating points. This is done by splitting the value range of each relevant parameter p into a number of characteristic intervals, n_p, using a graphic-based two-step approach based on the cumulative parameter curve. The process is illustrated in Figure 5 with power price chosen as parameter.

a) **Important values**: Some parameter values may be of special interest, making it relevant to introduce a break at these points. For instance, for the power price example, it may be relevant to introduce a break at a power price of 0.00 Euro/MWh to make sure that negative prices are grouped together. Also, if an operating decision, e.g. turning on a piece of equipment, is dependent on a given power price, an interval break should be introduced at this price as well.

b) **Even division**: If the already set break-points are far from each other in terms of both parameter value and duration, it is suggested that additional interval breaks are introduced to minimize the span. The break-points should be located such that the parameter value range is constant for each of the intervals.

3: Cluster procedure

Having defined the clustering criteria, the final step is to cluster the data in order to establish the final CHOP-groups G_i to replace the initial dataset of operating points O_j. Each G_i is characterised by a unique combination of characteristic parameter intervals, causing the maximum number of CHOP-groups to be:

$$N_{CHOP,max} = \prod_p n_p \tag{2}$$

All initial operating points O_j are sorted into the CHOP groups G_i based on parameter values. Any G_i with no O_j belonging to it is discarded. Each included G_i becomes an operating point in the final CHOP-reduced dataset characterised by a duration t_i (the sum of durations of the aggregated data points), a present value factor $t_{PV,i}$, and a number of operating condition parameters $\boldsymbol{p_i}$, which are the weighted average parameter values of the aggregated data points.

$$G_i = \{t_i, t_{PV,i}, \boldsymbol{p_i}\} \tag{3}$$

$$t_i = \sum_{O_j \in G_i} t_j \quad (4)$$

$$t_{PV,i} = \sum_{O_j \in G_i} \frac{t_j}{(1+i)^{Y_j}} \quad (5)$$

$$\boldsymbol{p_i} = \frac{\sum_{O_j \in G_i} \boldsymbol{p_j} \cdot t_j}{t_i} \quad (6)$$

with i being the annual discount rate.

If investment planning is not taken into account, a single CHOP-reduced dataset can be used for representing operating conditions over the lifetime of the FMG to be designed. In case investment planning is to be considered, one has to define a number intervals at the end of which novel investments are allowed, e.g. every 5th year, as suggested by Liu et al. [18]. If so, individual CHOP dataset must be developed for each investment interval, increasing the overall number of periods significantly in the final optimization model.

2.2.2. Surrogate modelling

In the design methodology, process and market models are reduced to step-wise linearized surrogate models in order to fit them into the optimization model developed. A generic illustration of a surrogate process model $K(\sigma_k, \lambda_{k,i})$, defined by a dimension σ_k and load $\lambda_{k,i}$, is presented in Figure 6.

Each surrogate process model $K(\sigma_k, \lambda_{k,i})$ is characterized by: A number of mass flows into the process $\boldsymbol{\dot{m}_{in,k}}(\sigma_k, \lambda_{k,i})$, and mass flows out of the process $\boldsymbol{\dot{m}_{out,k}}(\sigma_k, \lambda_{k,i})$; a number of internal thermal energy flows $\boldsymbol{\dot{e}_{internal,k}}(\sigma_k, \lambda_{k,i})$, thermal energy flows into the process $\boldsymbol{\dot{e}_{in,k}}(\sigma_k, \lambda_{k,i})$, and thermal energy flows out of the process $\boldsymbol{\dot{e}_{out,k}}(\sigma_k, \lambda_{k,i})$; plus investment costs $C_{inv,k}(\sigma)$ and operating costs $c_{op,k}(\sigma, \lambda)$. Furthermore, dimensional and operational constraints may be associated with each $K(\sigma_k, \lambda_{k,i})$. Each mass flow function $\dot{m}_{f,i}(\sigma_k, \lambda_{k,i})$ and operating cost function $c_{op,k}(\sigma_k, \lambda_{k,i})$ must be a linear or step-wise linear function of the load $\lambda_{k,i}$ as defined in equations (7) and (8). Each thermal energy flow function $\dot{e}_{f,i}(\sigma_k, \lambda_{k,i})$ is characterized by an inlet temperature $T_{in,f}$, an outlet temperature $T_{out,f}$, and a heat flow capacity

346 $C\dot{P}_{f,\iota}(\sigma_k, \lambda_{k,i})$ as defined in equation (9), with the latter being a linear or step-wise linear function of the

347 load $\lambda_{k,i}$ as defined in equation (10).

348 $$\dot{m}_{f,i}(\sigma_k, \lambda_{k,i}) = \boldsymbol{f_{linear}}(\sigma_k, \lambda_{k,i}) = \begin{cases} \sigma_k(a_1\lambda_{k,i} + b_1) & , \lambda_{k,i}\epsilon I_1 \\ \sigma_k(a_2\lambda_{k,i} + b_2) & , \lambda_{k,i}\epsilon I_2 \\ \dots \end{cases} \quad (7)$$

349 $$c_{op,k}(\sigma_k, \lambda_{k,i}) = \boldsymbol{f_{linear}}(\sigma_k, \lambda_{k,i}) = \begin{cases} \sigma_k(c_1\lambda_{k,i} + d_1) & , \lambda_{k,i}\epsilon I_1 \\ \sigma_k(c_2\lambda_{k,i} + d_2) & , \lambda_{k,i}\epsilon I_2 \\ \dots \end{cases} \quad (8)$$

350 $$\dot{e}_{f,i}(\sigma_k, \lambda_{k,i}) = \{\dot{CP}_f(\sigma_k, \lambda_{k,i}), T_{in,f}, T_{out,f}\} \quad (9)$$

351 $$\dot{CP}_{f,i}(\sigma_k, \lambda_{k,i}) = \boldsymbol{f_{linear}}(\sigma_k, \lambda_{k,i}) = \begin{cases} \sigma_k(g_1\lambda_{k,i} + h_1) & , \lambda_{k,i}\epsilon I_1 \\ \sigma_k(g_2\lambda_{k,i} + h_2) & , \lambda_{k,i}\epsilon I_2 \\ \dots \end{cases} \quad (10)$$

352 In the equations, $I_1, I_2, \dots$ are the load intervals for which the step-wise linear functions apply, while

353 $\{a, b, c, d, g, h\}$ represent linear function constants. Note that power flows are modelled as mass flows as

354 they do not require quality differentiation in process integration methods.

355 To represent possible economy of scale effects, power laws [51] are used to calculate investment costs

356 $C_{inv,k}(\sigma_k)$ of the surrogate process models as a function of the dimension σ_k and a scaling constant $M_{f,k}$:

357 $$C_{inv,k}(\sigma_k) = C_{inv,k0}\left(\frac{\sigma_k}{\sigma_{k0}}\right)^{\mathrm{M_{f,k}}} \quad (11)$$

358 with $C_{inv,k0}$ being the reference investment cost and σ_{k0} the reference dimension of the process K.

359 Multiple process models may be merged into combined surrogate models if they are synchronized, i.e. their

360 dimensions are aligned and they share the same load pattern at all times. Processes with non-synchronised

361 dimensions and load patterns must be assigned individual surrogate models.

362 A generic illustration of surrogate models for product or service markets, $R(\boldsymbol{\lambda_i})$, thermal energy markets

363 $R_{th}(\boldsymbol{\lambda_i})$, and local biomass markets $R_b(q_{b,an})$, which are functions of the FMG load vectors $\boldsymbol{\lambda_i}$, are

364 presented in Figure 7.

365 Each surrogate product market model R is characterized by: Mass flows of bought and sold products

366 $\dot{m}_{bought}(\boldsymbol{\lambda})$, $\dot{m}_{sold}(\boldsymbol{\lambda})$; product price as a function of FMG operation $c(\boldsymbol{\lambda})$; and production and demand

constraints. Each surrogate thermal energy market model R_{th} is characterised by: Forward and return thermal energy flows $\dot{e}_{forward}(\boldsymbol{\lambda})$, $\dot{e}_{return}(\boldsymbol{\lambda})$; thermal energy service price as a function of FMG operation $c_{th}(\boldsymbol{\lambda})$; temperatures of the thermal flows $T_{forward}$, T_{return}; and generation and demand constraints. Each surrogate local biomass market model is characterized by a mass flow of biomass $\dot{m}_b(q_{b,an})$ and a vector of marginal biomass costs $\boldsymbol{c_b}(q_{b,an})$ as functions of the annual biomass demand $q_{b,an}$, as described in more detail in Section 2.2.3.

2.2.3. Biomass supply chain modelling

If local biomass resources are to be consumed, a biomass supply chain model must be established to relate the marginal biomass unit cost to the biomass feedstock consumption. As discussed by e.g. Jack [50] and Boldrin et al. [52], transportation costs may be central of the economic analysis of local biomass resources. In the present methodology, a generic biomass supply chain model is integrated analogous to the one developed for sugar beet by Boldrin et al. [52].

In the model, the biomass unit cost $c_b(q_{b,an})$ as a function of the annual biomass quantity demanded $q_{b,an}$ is assumed to consist of two components, namely a reference cost c_{b0} and a cost for transportation, $c_{b,tr}(q_{b,an})$. The reference cost is a fixed cost representing the price paid to the local farmers for the biomass, while the transportation cost represents the variable costs of logistics for delivering biomass to the FMG.

$$c_b(q_{b,an}) = c_{b0} + c_{b,tr}(q_{b,an}) \tag{12}$$

In order to calculate $c_{b,tr}(q_{b,an})$, the land around the FMG is assumed divided as illustrated in Figure 8. It is assumed that the transportation cost for all biomass cultivated in an area A_h is constant and equal to the cost of transporting the biomass the mean transportation distance $d_{tr,h}$, which is calculated as

$$d_{tr,a} = r_{a-1} + \left(\frac{r_a - r_{a-1}}{\sqrt{2}}\right) \tag{13}$$

The marginal biomass unit cost $c_b(q_{an})$ is then calculated as

$$\boldsymbol{c_b}(q_{b,an}) = c_{b,ref} + \begin{cases} c_{trans,1}(d_{tr,1}) \mid q_{b,an} \in [0; q_1] \\ c_{trans,2}(d_{tr,2}) \mid q_{b,an} \in]q_1; q_1 + q_2] \\ \dots \\ c_{trans,a}(d_{tr,a}) \mid q_{b,an} \in]\sum_{a-1} q_a ; \sum_i q_a] \end{cases} \quad (14)$$

The annual biomass cultivation q_a in each area A_a is calculated from the input data on local resources. The identified marginal biomass costs are included in the CHOP-reduced dataset for external operating conditions. This implies that any variation in the marginal biomass costs over the seasons or years can be taken into account in the optimization model. If several local biomass feedstocks are considered for processing, multiple BCM models can be defined in the design methodology.

2.3. Optimization phase

The optimization phase of the design methodology is based on a genetic algorithm and a multi-period mixed integer-linear programming (MILP) model from the OSMOSE software [48], which is developed at École Polytechnique Fédérale de Lausanne, Industrial Process and Energy Systems Engineering lab. In short, the optimization phase consists of three steps: 1. A genetic algorithm, used for selecting, locating, and dimensioning processes to be included in an FMG, and deciding upon possible investment plans; 2. a multi-period MILP model for optimizing process integration and operation of the given processes over the lifetime of the facility, and 3. a post calculation step for calculating the overarching objective function values of each optimized design. The calculated objective function values are provided as feedback to the genetic algorithm. The three steps are described in detail below.

2.3.1. Genetic algorithm

A genetic algorithm developed at EPFL [48] is used for selecting, locating and dimensioning processes to be included in the FMG, and for determining the strategy if investment planning is considered. The genetic algorithm is preferred as the master optimization algorithm as it can be used for solving linear as well as non-linear models and is capable of conducting multi-objective optimization [53].

In short, a genetic algorithm is a heuristic optimization algorithm that imitates the process of natural selection for solving an optimization problem. The variables of the optimization problem are seen as 'genes', while the objective function or functions describe the 'Darwinian fitness' of a solution. To start with, a population of a defined number of solutions with randomly assigned genes is generated, and the fitness of each solution is assessed. Next, a second population is 'bred' from a *selected* number of well-performing 'parent' solutions from the first population. The new solutions inherit genes from the parent solutions as defined by the genetic operator *crossover*, while some of the inherited genes may be altered by the genetic operator called *mutation*. The genetic algorithm then iterates over a defined number of generations in search for optimal combinations of genes.

When running the genetic algorithm in OSMOSE, one defines the population size and number of generations, while the algorithm has pre-defined settings for selection, mutation, and crossover [48]. For general information on genetic algorithms, consult e.g. [54].

The objectives of the genetic algorithm are to minimize the negative net present value $NPV(\boldsymbol{\omega}, \boldsymbol{\sigma}, \boldsymbol{y})$ and the global warming potential $GWP100a(\boldsymbol{\omega}, \boldsymbol{\sigma}, \boldsymbol{y})$. Variables considered are ω_k, the decision of whether or not a process or piece of equipment k should be installed at a given location; σ_k, the dimension of k; and y_k, the installation delay of k in years. The optimization problem to be solved by the genetic algorithm in the design methodology can be written in condensed form as

$$\begin{cases} \min_{\boldsymbol{\omega},\boldsymbol{\sigma},\boldsymbol{IP}} \begin{cases} -NPV(\boldsymbol{\omega}, \boldsymbol{\sigma}, \boldsymbol{y}) \\ GWP100a(\boldsymbol{\omega}, \boldsymbol{\sigma}, \boldsymbol{y}) \end{cases} \\ \text{with variables} \\ \omega_k \in \{0,1\} \\ \sigma_k \in [\sigma_{k,min}, \sigma_{k,max}] \\ y_k \end{cases} \tag{15}$$

Infrastructure for connecting facility locations is dimensioned by the genetic algorithm as well. The methodology is therefore not advantageous for systems with a large number of location options. Back-up utility processes are not dimensioned by the genetic algorithm, but by the MILP model based on required maximum capacities over the expected operating pattern.

2.3.2. Mixed integer-linear programming model

Given the selection and location $\boldsymbol{\omega}$, the dimension $\boldsymbol{\sigma}$, and the time of instalment $\boldsymbol{y}$ for all processes k, process integration and operation optimization over the lifetime of the FMG can be conducted. In order to reduce computation time and to guarantee that global optimality is reached for the operation optimization, a multi-period mixed integer-linear programming (MILP) model [48] is established to minimize operation costs $c_{op,i}(\boldsymbol{\nu_i}, \boldsymbol{\lambda_i})$ of the given FMG layout in each CHOP group i, which in total represents operation optimization over the lifetime of the facility. The variables are: $\nu_{k,i}$, the decision on whether a process k is running or shut down in period i; and $\lambda_{k,i}$, the load of the process if it is running.

The MILP model is constructed so that each type of mass flow in the system has its own layer l. Mass balance applies for each layer over each period i and is included as a constraint in the MILP model.

$$\sum \dot{m}_{f,l,i} = 0 \tag{16}$$

Special layers are constructed for thermal energy flows, for which pinch analysis [55] is applied to optimize heat integration. As heat integration over geographical distances may not be feasible, a thermal energy layer must be defined for each area within which heat integration is feasible. If all facilities considered in an FMG are co-located, it may be sufficient to define a single thermal energy layer.

As mentioned previously, hot and cold thermal energy flows $\dot{\boldsymbol{e}}(\boldsymbol{\sigma}, \boldsymbol{\lambda_i})$ from processes and markets are assumed to have step-wise constant heat capacity flow rates $\dot{\boldsymbol{CP}}(\boldsymbol{\sigma}, \boldsymbol{\lambda_i})$ over their temperature ranges. Assuming a pinch temperature difference of 10K, the temperatures of hot streams are shifted 5K up and the temperatures of cold streams are shifted 5K down. For each thermal layer in the FMG model, enthalpy balances ΔH are calculated for each temperature interval s:

$$\Delta H_{s,i} = (T_s - T_{s-1}) \sum_s \dot{CP}_s(\boldsymbol{\sigma}, \boldsymbol{\lambda_i}) \tag{17}$$

To satisfy the first law of thermodynamics, the sum of all temperature interval enthalpy flows in each thermal energy layer must be zero. Furthermore, the sum of enthalpy flows from the first temperature interval to any of the other temperature interval in each thermal energy layer must never be below zero to make sure that the 2nd law of thermodynamics is satisfied:

458 $$\sum \Delta H_{s,i} = 0 \quad (18)$$

459 $$\sum_{s=1}^{m} \Delta H_{s,i} \geq 0 \quad \forall\ m \in \{1,2,\dots,s_{max}\} \quad (19)$$

460 The optimization problem to be solved by the MILP model in the design methodology can be written in
461 condensed form as

462 $$\begin{cases} \text{given } (\boldsymbol{\omega}, \boldsymbol{\sigma}, \boldsymbol{y}) \\ \min_{\boldsymbol{\lambda_i}, \boldsymbol{\nu_i}} c_{op,i}(\boldsymbol{\nu_i}, \boldsymbol{\lambda_i}) \\ \text{with variables} \\ \nu_{k,i} \in \{0,1\} \\ \lambda_{k,i} \in [\lambda_{k,min}, \lambda_{k,max}] \\ \text{and constraints} \\ (16), (18), (19) \\ load\ and\ demand\ constraints \end{cases} \quad (20)$$

463 Once the MILP model has been solved, the global warming impact of the optimized operation $z_{op,i}(\boldsymbol{\nu_i}, \boldsymbol{\lambda_i})$
464 is calculated for each period i.

465 In OSMOSE [48], the required investment in heat exchangers $C_{HEN,i}$ is estimated as a part of the pinch
466 analysis for each operating mode i using a method from [56]. For more information, consult Bolliger [48].
467 In the MILP model, no constraint is put on the dimensions of utility services $\boldsymbol{\sigma_{ut}}$ in order to make sure that
468 constraints (17) and (18) are satisfied at all operating points. Once the MILP model has been solved, $\boldsymbol{\sigma_{ut}}$ is
469 identified as the largest required utility service demand experienced over the lifetime of the system, and
470 the investment cost is calculated using the power law function given in equation (11).

471 ### 2.3.3. Post computation

472 Once the MILP operation optimization has been conducted, a post-calculation step is used for evaluating
473 the overall performance of the optimized FMG with respect to NPV and GWP100a.
474 First, the heat exchanger network investment cost, C_{HEN}, is defined as the largest estimated heat
475 exchanger investment cost as identified by OSMOSE [48]:

476 $$C_{HEN} = \max_i C_{HEN,i} \quad (21)$$

477 The NPV, C_0, of the design is calculated as

$$C_0 = -\left[C_{HEN} + \sum_k \frac{C_{inv,k}(\sigma_k)}{(1+i)^{y_k}}\right] - \sum_i c_{op,i} \cdot t_{PV,i} \quad (22)$$

with y_{lt} being the facility lifetime and i the annual discount rate.

The global warming potential Z_0 of the design is calculated as

$$Z_0 = z_{inv,HEN} + \sum_k z_{inv,k}(\sigma_k) + \sum_i z_{op,i}(\boldsymbol{\nu_i}, \boldsymbol{\lambda_i}) \cdot t_i \quad (23)$$

Here, $z_{inv,HEN}$ is the global warming potential related to the production, installation, and scraping of the heat exchanger network, $z_{inv,k}(\sigma_k)$ is the global warming potential related to the production, installation, and scraping of the process $K(\sigma_k)$, and $z_{op,i}(\boldsymbol{\nu_i}, \boldsymbol{\lambda_i}) \cdot t_i$ is the overall global warming potential of the FMG operation in period i.

The calculated NPV and GWP100a are provided as feedback to the genetic algorithm. All data on optimized designs are stored in a database for later evaluation.

2.4. Evaluation phase

2.4.1. Pareto assembly

Following the optimization phase, a Pareto frontier is assembled for optimized design solutions with respect to the two objectives, NPV and GWP100a. The Pareto frontier illustrates the border between the feasible solution space and the infeasible solution space of the optimization problem. Designs placed on the Pareto frontier are called efficient designs, as they represent the optimal pay-off between the two objectives of the optimization problem. An example of a Pareto frontier is developed as a part of the case study in Section 3 and can be seen in Figure 11.

2.4.2. Sensitivity analysis and uncertainty analysis

Design optimization of FMGs involves many sources of uncertainty, e.g. technology learning curves, energy system development, policy schemes, estimated investment, operating costs etc. It is therefore important to assess variations in the performance of optimized designs as functions of input data uncertainty. In the present design methodology, uncertainties with respect to external operating conditions (energy systems)

are considered by solving the developed optimization problem for various scenarios, while uncertainties of economic and environmental parameters are considered for a number of selected designs in each scenario using the following three-step procedure for assessing output uncertainty:

1. Selection of a number of interesting designs.
2. Morris screening [57] is applied on each selected design for assessing the relative impact on performance variability from input parameter uncertainty.
3. Monte Carlo simulation is applied for quantifying performance variability of each selected design.

Uncertainties regarding topological parameters, such as equipment failure or forced outages, are not considered in the design methodology.

Morris screening: Extended Morris screening [57][58] is a global sensitivity analysis method that is applied for assessing how the various input data uncertainties affect variations in model outputs. The method relies on estimation of elementary effect EE on each model output from each input parameter p. The main advantage of Morris screening is its low computational cost when compared to other global sensitivity analysis methods. The method uses a special sampling technique, Morris sampling, and it has two degrees of freedom to be specified by the user: b, the number of value levels that an uncertain input parameter can take within its range; and w, the number of elementary effects to be calculated for each input in order to identify the elementary effect distributions $\boldsymbol{D}_{\boldsymbol{EE},p_y}$ for each parameter p_y on each output function f.

The elementary effect vector $\boldsymbol{EE}_{p_y}$ for a parameter p_y is calculated as:

$$\boldsymbol{EE}_{p_y} = \frac{\boldsymbol{f}(p_1,p_2,\dots,p_y+\Delta,\dots,p_M)}{\Delta} \tag{24}$$

Here, $\boldsymbol{f}(p)$ are model output functions, and M is the total number of uncertain model parameters considered. Δ, a perturbation factor for the input parameters, is optimal when calculated as:

$$\Delta = \frac{p}{2(p-1)} \tag{25}$$

Once all EE_{ij} have been calculated for w random samples of input parameters, sigma-scaling [58] of EE_{p_y} is applied so that the impacts of input parameters on various outputs can be compared:

$$SEE_{p_y,f} = EE_{ij} \frac{(standard\ deviation)_{p_y}}{(standard\ deviation)_f} \quad (26)$$

Here, $(standard\ deviation)_{p_y}$ is the standard deviation of the input parameter p_y, while $(standard\ deviation)_f$ is the standard deviation of the output f from simulation results.

Based on the simulation results, the means and standard deviations of all sigma-scaled elementary effects $\boldsymbol{SEE}_{p_y}$ are calculated and assembled in scatter plots. In each plot, two lines corresponding to the positive and negative double estimated standard error of the mean, $mean_i$, are drawn:

$$mean_i = \pm 2 \cdot \frac{standard\ deviation_i}{\sqrt{w}} \quad (27)$$

As described by Sin et al. [58], these lines may be used for dividing uncertain input parameters into significant or negligible with respect to model output variation. If the elementary effect of a parameter falls within the two lines, its impact can be interpreted as negligible on the model output variation.

An example of the application of Morris screening and interpretation of its results is given in the case study in Section 3.

Monte Carlo simulation: Following the Morris screening, the Monte Carlo simulation procedure presented by Sin et al. [58] is applied for quantifying the overall model output variation with respect to each of the two performance objectives. The Monte Carlo simulation is a technique for investigating output variability through uncertainty sampling and probability statistics. It has been chosen for the design methodology as it may provide uncertainty results without necessitating modifications or manipulations of the original models and because it facilitates identification of nonlinearities, thresholds, and discontinuities [59]. The procedure applied in the design methodology involves three steps:

1. *Specifying input uncertainty*: In general, the Monte Carlo simulations may consider uncertainty distributions D for all input data. However, in order to reduce the number of parameter distributions to sample from, the parameters identified to have insignificant impact on model output variability in the Morris screening are not considered in the input uncertainty for the Monte Carlo simulations.

2. *Sampling from input uncertainty*: In order to obtain dense stratification over the range of each sampled variable without having to define the stratification manually, the Latin Hypercube Sampling method [60] is applied for sampling from input uncertainty.
3. *Evaluating the model for sampled input uncertainty*: The optimization model is run for all sampled datasets. The Monte Carlo results provide a cumulative distribution function of the output functions which may be evaluated using basic statistics.

2.5. Outputs

The design methodology yields two overall outputs:

1. An assembled Pareto curve and a database of feasible designs that have been optimized with respect to NPV and GWP100a.
2. For selected designs:
    a. The sigma-scaled elementary effect of each input parameter p on each model output.
    b. A quantification of model output variation as a function of input uncertainty.

To demonstrate the use of the design methodology, it is applied in a case study in Section 3.

3. Case study: Conceptual FMG

In this section, the developed design methodology is applied in a simple case study which treats the retrofit of an existing combined cycle combined heat and power (CHP) plant. With the aim of strengthening the integration between layers of the energy system, a number of routes for converting local biomass into power, heating, fuels, and other products are considered for integration in the CHP plant, and the impact of such integration on the overall economic and environmental performance of the plant is then assessed. The retrofit options considered include the possible installation of: A straw-based cellulosic ethanol production facility based on IBUS technology [61]; a biomethane facility, which includes an anaerobic digester producing biogas from manure, industrial waste, and ethanol production molasses, with an integrated

biogas upgrading facility; a biomass boiler and a natural gas boiler for utility heat; and a ground-based compression heat pump for district heating generation. A superstructure of possible retrofit options is presented in Figure 9. All processes are assumed to be co-located, while investment planning is neglected. A preliminary version of the case study was presented in [62].

3.1. Input data and structuring

3.1.1. Surrogate process models

A surrogate model of a gas turbine (GT) and a bottoming steam Rankine cycle (SR) were developed based on data from the Danish back-pressure combined cycle CHP plant 'Silkeborg Kraftvarmeværk' [63]. In the surrogate models, temperature levels were assumed to be load-independent, while gas consumption, GT power generation, and off-gasses heat flow capacity were assumed to be directly proportional to the GT load λ_{GT}. The heat and power generation of the SR were assumed directly proportional to the SR load λ_{SR}. Both the GT and the SR were assumed to operate adiabatically. Data used for developing the GT and SR surrogate models are presented in Table 1.

A surrogate model of an IBUS ethanol facility (IB) was developed based on a validated IBUS facility model by Lythcke-Jørgensen et al. [14][64], with the modification that thermal separation stages were replaced by mechanical separation stages. A surrogate model of a biomethane facility (AD), consisting of a thermophilic anaerobic digestion reactor operating at 55°C and a biogas upgrading facility, was developed based on models presented by Evald et al. [65]. The IB and the AD were assumed to have zero load flexibility.

Surrogate models of a gas boiler (GB), a biomass boiler (BB), and a district heating heat pump (HP) were developed based on data presented by the Danish Energy Agency [66].

Economic data on the surrogate models are presented in Table 2. In the calculations, a plant lifetime of $y_{lt} = 30\ years$ and an annual discount rate of $i = 0.06$ were assumed. For power law investment calculations as defined in equation (11), an investment scaling constant of $M_f = 0.75$ was used.

595 Thermal energy flows as functions of process variables are presented in Table 3. It was assumed that a cold
596 water reservoir with a temperature of 15°C was available for balancing heat flows in the system. As all
597 processes were considered to be co-located, a single thermal energy layer was defined in the model.

598 Mass flows in the various layers as functions of process variables are presented in Tables 4-8. Note that
599 power flows were modelled as mass flows in a separate layer. Market surrogate models were introduced
600 into each layer to ensure mass balances.

601 3.1.2. Energy system, market, and environmental impact data

602 For the case study, the power price c_{el} and the relative district heating demand λ_{DH} were identified as
603 relevant external operating parameters. A CHOP-reduced dataset of c_{el} and $\lambda_{DH,ref}$ based on historical
604 data for western Denmark over the period primo 2010-ultimo 2014 has been presented by Lythcke-
605 Jørgensen et al. [49]. This dataset was applied in the present case study as representative for operating
606 conditions over the lifetime of the studied FMG. The CHOP-reduced dataset is presented in Tables 9-12. A
607 scatter plot of original and reduced operating condition data points is presented in Figure 10.
608 For simplicity, the environmental objective of the study only considered CO_2-emissions from facility
609 production and avoided CO_2-emissions from displaced external production. Average emission values were
610 in general applied for the displaced production. Marginal values may, however, be utilised, e.g. in
611 combination with energy system analysis [67]. Economic and environmental data on consumed and sold
612 products are presented in Table 13. Biomass was assumed to be CO_2 neutral. Manure was assumed to be
613 delivered free of charge by local farmers in exchange for free, digested fertilizer. Manure emission impacts
614 were not considered, although anaerobic digestion of manure may reduce greenhouse gas emissions
615 significantly as compared to conventional use of undigested manure as fertilizer.

616 3.1.3. Biomass supply chain model

617 Apart from the straw cost paid to the producers as indicated in Table 13, an additional cost was placed on
618 straw import to represent costs for transport and logistics. The company EA Energy Analysis [73] has

reported a fixed cost of 1.07 Euro/GJ for straw logistics in Denmark, including transportation for up to 10 km, while an additional cost of 0.009 Euro/(GJ/km) is charged for every additional kilometre. Assuming a mean winter wheat straw yield of 4,183 kg/ha, as suggested by Bentsen et al. [74], and that 20% of the area around the facility has winter wheat cultivation, a surrogate biomass supply chain model was developed. The model is presented in Table 14. It was not assumed feasible to import biomass from outside the 50 km radius area around the facility.

3.1.4. Optimization constraints

Design variables and constraints in the case study are summarized in Table 15. As previously mentioned, investment planning was not considered in the present case.

Operation variables and constraints are summarized in Table 16 and equation (28). As the GB was considered a back-up utility, it was dimensioned in the operation optimization step based on maximum required load. Note that the ethanol facility and the combined biogas facility were assumed to be inflexible, implying that load variations are not considered in the operation optimization. The facility was considered to be the sole provider of heating for the district heating grid, and, consequently, the district heating generation must meet the demand at all times.

$$\lambda_{DH} \equiv \lambda_{DH,ref} \tag{28}$$

In the optimization phase, the genetic algorithm was run for a population size of 50 over 5 generations.

3.1.5. Sensitivity and uncertainty analysis

The uncertain input parameters considered in the case study and their distributions are given in Table 17.

The reference investment costs and the ethanol price were given a relative uncertainty of $\pm 25\%$ with a uniform distribution to represent cost and market uncertainties. The CO_2 emissions displaced from the ethanol produced z_{eth} was assumed to vary in the range $[0\%, -40\%]$ with a uniform distribution to represent the facts that it may not be gasoline that is replaced by the produced ethanol, and that the straw

642 consumed may not be CO_2 neutral. Finally, the investment scaling constant was given an uncertainty range
643 of $[0.6,0.9]$ with a uniform distribution to represent the uncertainties related to the economy of scale
644 benefits from investments.

645 Morris screening was conducted with $\{b, w\} = \{8,35\}$. For each Monte Carlo simulation, a sample of 250
646 data points was generated using Latin Hypercube Sampling [60] and assuming zero correlation between
647 uncertainties in input parameters.

648 3.2. Results and evaluation

649 A database of feasible designs with optimized operation was obtained from running the optimization model.
650 A scatter plot of the optimized designs with respect to NPV and CO_2 emission impact is shown in Figure 11.
651 In general, it was found that the larger the dimension of the biomass treatment facilities, the lower the NPV
652 and the lower the total CO_2 emission impact, illustrating the cost of avoided CO_2 emissions in the case study.
653 It was further found that the cost of avoided CO_2 emission was higher for designs including both ethanol
654 and biomethane production than for designs with only ethanol production. This trend is primarily caused by
655 two effects: First of all, avoided CH_4 emissions from undigested manure were not considered in the
656 calculations, which would expectedly reduce the total CO_2 emission impacts from designs with biogas
657 production significantly. Secondly, a GB was installed as back-up utility heat source, and it was used in
658 periods where it was economically unfavourable to operate the gas turbine while power for running the
659 operation was imported from the grid. Combined, this made the overall biomethane production
660 unfavourable from both an economic and an environmental perspective in the case study.
661 The results further indicate that the NPV is reduced while the CO_2 emission impact is only slightly affected
662 for larger biomass boiler dimensions, suggesting that the biomass boiler is hardly used in the operation
663 optimization for economic reasons. This opposes the current (2015) trend in Denmark where biomass,
664 which is currently tax free, is replacing the taxed natural gas in the heating sector. The reason for this
665 difference is the fact that tax and subsidy schemes are not considered in the calculations. The results also

suggest that operation with a district heating heat pump is favourable for specific periods, but that the investment costs make the overall economic performance of heat pumps unfavourable. Again, it must be stressed that taxes and subsidy schemes were not considered in the calculations.

Three interesting designs, *I*, *II*, and *III*, were chosen for further investigation. Here, *I* is the identified retrofit design with the highest NPV; *II* is the identified retrofit design with the lowest CO_2-emission impact; and *III* is the retrofit design with the largest NPV that includes biomethane production. The characteristics of the designs are described in Table 18, together with the performance of the reference facility (Ref).

Based on the input parameter uncertainties defined in Table 17, Morris screening was applied for identifying elementary effects on NPV and GWP100a from each of the uncertain input parameters in each of the three selected designs. An example of an elementary effect histogram obtained using Morris screening is plotted in Figure 12.

The means and standard deviation of the sigma-scaled elementary effects from uncertain input parameters on each of the model outputs are plotted for the three selected designs in Figure 13. The wedges in the figures represent the standard error of the mean as defined in equation (25). Elementary effects with mean and standard deviations of zero are not labelled in the figures.

The scatter plots illustrate the relative importance of each of the input parameter uncertainties on each of the model outputs. From Figure 13, it is seen that the NPV of design *I* would be significantly affected by uncertainties in reference ethanol facility investment cost $C_{inv,IB0}$ and investment scaling constant M_f, as the mean and standard deviations of their elementary effects' on NPV are far outside the standard-error-of-the-mean wedge. Furthermore, it is seen that the impacts of $C_{inv,IB0}$ and M_f are either correlated with other uncertain input parameters, non-linear, or both, as their standard deviations are different from zero. The ethanol price c_{eth} on the other hand was found to have a linear impact on NPV as the elementary effect has a standard deviation of zero. These observations can easily be confirmed by investigating the model structure. It is further seen that the NPV of design *I* was neither affected by the displaced CO_2

690 emission from ethanol z_{eth} nor the reference investment costs of the biomethane facility $C_{inv,AD0}$ and
691 district heating heat pump $C_{inv,HP0}$. This is evident from the fact that the dimension of the heat pump was
692 negligible, no combined biogas facility was installed, and no economic cost was associated with CO_2
693 emissions. Opposed to this, as expected, z_{eth} is found to be the only parameter affecting the total CO_2
694 emission impact.

695 Similarly, observations on impact of parameter uncertainties were made for designs *II* and *III* based on
696 Figure 13. For *II*, it was found that c_{eth} had significantly more impact than the other designs. This is due to
697 the fact that the ethanol facility was markedly larger, causing ethanol sales to have a relatively larger
698 impact on the NPV. For *III*, it was found that $C_{inv,AD0}$ was no longer negligible, as a biomethane facility was
699 in fact installed.
700 Based on the Morris screening results, Monte Carlo simulations were conducted for each of the three
701 designs considering non-negligible uncertainties in input parameters. The parameters considered are
702 summarized in Table 19. The Latin Hypercube Sampling method was applied for generating samples of each
703 250 data points for use in the Monte Carlo simulations. A visual representation of the Latin Hypercube
704 sample used in the Monte Carlo simulation for design *I* is presented in Figure 14.

705 Running Monte Carlo simulations for each of the three selected designs, the resulting 10^{th} to 90^{th} percentile
706 interval of predicted NPV and 0^{th} to 90^{th} percentile interval of predicted GWP100a are indicated for each of
707 the three selected designs in Figure 15.

708 The figure illustrates the variability in performance of the selected designs as functions of the defined input
709 uncertainty. It is seen how the NPV variation is somewhat evenly distributed around the predicted value,
710 which is to be expected as uncertainties in economic parameters are all considered to be evenly and
711 uniformly distributed around the reference value. It is furthermore seen that the predicted CO_2 emission
712 impact in the deterministic run is the lowest possible as the considered uncertainties in CO_2 emission
713 impact can only lead to higher CO_2 emission impacts.

In general, the performance variations are found to be larger for design *II*, caused by larger retrofit investments and a larger ethanol production, implying that the relative uncertainties in investments, ethanol prices and replaced CO_2 emissions from produced ethanol will have a larger impact in absolute terms.

Even with 10^{th} to 90^{th} percentile intervals, design *I* will outperform design *III* with respect to NPV, whereas the total CO_2 emission impact is somewhat similar, suggesting that *III* should not be selected for the given case. Considering the found performance intervals, design *I* has a CO_2 reduction price of 4.9-30.3 Euro/ton, while design *II* has a CO_2 reduction price of 8.4-32.1 Euro/ton. Hence, in the marginal case, the results suggest that design *I* should be preferred if cost-efficient CO_2 reductions are desired.

A central aspect of the design methodology is the application of systematic process integration. To assess the importance of this feature, the performances of each of the three selected designs were evaluated without consideration of process integration, i.e. the combined cycle CHP and the biomass treatment facilities were operated separately. The change in performance is illustrated in Figure 16.

It is clear that without process integration, all three designs obtained lower NPV and higher CO_2 emission impacts. Also, it appears that the larger the dimensions of the biomass processing equipment, the larger the absolute reduction in performance. Altogether, this demonstrates the importance of considering process integration, both when developing smart energy systems in general and when designing FMGs in particular.

4. Discussion and perspective

This paper presents a generic methodology for optimizing the design of flexible multi-generation systems (FMGs), which are systems consisting of integrated and flexibly operated facilities that together provide multiple links between layers of the energy system.

One of the challenges of the presented design methodology is the fact that it is based on partial analysis, which implies that the impact on system level of FMG operation is neglected. However, as the central hypotheses for FMGs consider impacts on system levels, it is crucial that the aggregated impact of FMGs is assessed. For instance, if a number of FMGs are set to balance the power system by generating electricity in periods with no generation from renewable sources, they may become market dominating and thereby affect the power prices - a situation that makes partial analysis insufficient. One way of assessing the aggregated impact of FMG operation is to apply the developed design methodology for identification of preliminary designs of FMGs, and then integrate these designs in an energy system model in order to assess the system impact. The results from the energy system analysis could then be provided as feedback to the design methodology in an iterative loop. This topic will be treated in future research by the group.

One of the shortcomings of the design methodology is the fact that thermal storages and dynamic operation constraints cannot be considered due to the application of the CHOP method [49]. The latter is applied to reduce computation times when searching for optimal designs while still maintaining detailed information on flexible operating conditions, which was previously proven to be crucial for obtaining optimal designs [62]. An advantage of the CHOP method is the fact that it is capable of capturing non-cyclic patterns in the energy system as opposed to most other energy system data aggregation methods, e.g. standard days, standard periods, average periods etc. [49]. To overcome the shortcoming of dynamic operation, the optimization phase of the methodology can be divided into two parts: A preliminary part where CHOP-reduced energy system data are used for the preliminary design, and a second part where chronological energy system data are used for detailed design and performance evaluation. This is analogous to the methodology presented by Rubio-Maya et al. [29], [30]. The second step would then allow for the consideration of thermal energy storages and dynamic operational constraints, albeit at the cost of increased computational time. Whether or not this is the right way to proceed is a relevant topic for further investigation.

In the design methodology, a genetic algorithm is used as the master algorithm to be able to digest all sorts of models and scan the solution space for efficient solutions. However, being heuristic by nature, it cannot guarantee optimality of the solutions. For example, in the simple case study considered, the optimized retrofit design with the highest NPV, 'I', had a biomass boiler of 1.1 MJ/s and a heat pump of 0.3 MJ/s installed, while the ethanol facility straw processing capacity was 5.2 kg/s. If the biomass boiler and heat pumps are removed, and the ethanol facility dimension is reduced to the minimum, i.e. 5.0 kg/s, the NPV would increase from 14.6 MEuro to 24.5 MEuro. This illustrates one of the drawbacks of using genetic algorithms: They may approximate the optimal or efficient solutions, but are not guaranteed to find them. However, as the present methodology is focussed on pre-feasibility studies of FMGs, the genetic algorithm is considered advantageous as it efficiently 'separates the wheat from the chaff'.

One of the novelties of the method is the consideration of local biomass supply chains, which is likely to have an impact on the dimensioning of biomass-processing FMGs [50]. In a similar manner, local industry and its demand for process heat, cooling, and other energy services ought to be considered when designing FMGs. If local industry is systematically considered for process integration in FMG studies, the overall energy and exergy efficiency of the local community may be increased further, and the industry demands may impact the dimensioning of FMGs as well. Thus, FMGs may be considered as supply facilities in local energy hubs or industrial symbioses, characterized by a high degree of mass and energy integration and reduced environmental impacts when compared to stand-alone industry.

In general, it is relevant to allow for future retrofit options when designing complex systems like FMGs, as discussed by Liu and Pistikopoulos [22]. However, inclusion of investment planning in the design methodology is challenging as both technological and system developments are hard to predict. Whether or not investment planning should be considered in pre-feasibility analysis depends on the case treated, but it is evident that the computational time would increase exponentially as multiple investment scenarios would have to be considered by the genetic algorithm.

784 Economic and environmental parameter uncertainties are efficiently handled in the design methodology
785 using a combined Morris screening/Monte Carlo simulation approach. With regard to handling of energy
786 system uncertainties in the design methodology, it is recommended that explorative scenarios are used to
787 give a better overview of optimality differences between likely, but fundamentally different, energy system
788 scenarios. It should be noted that the total computation time is approximately proportional to the number
789 of scenarios investigated in the developed design methodology. In the present study, it took approximately
790 84 hours to conduct all calculations on a laptop with an Intel® Core™ i7-3720QM CPU @ 2.60 GHz
791 considering one energy system scenario.
792 The present case study featured a socio-economic analysis as neither taxes nor subsidies were considered.
793 In general, socio-economic analyses can be used for providing recommendations for policy makers. If the
794 design methodology is used with the aim of guiding investment decisions, it would be relevant to conduct a
795 private economic evaluation including taxes and subsidies.
796 A significant outcome of the case study is the assessment of impact from systematic process integration in
797 the design methodology. The results show how the selected designs become suboptimal when process
798 integration is neglected, and thus underline the importance of including process integration when
799 developing smart energy systems in general and when designing FMGs in particular.

800 # 5. Conclusion

801 A generic methodology for optimizing the design of FMGs is presented which simultaneously consider the
802 following issues: Selection, location, and dimensioning of processes; systematic heat and mass integration;
803 flexible operation optimization with respect to both short-term market fluctuations and long-term energy
804 system development; global sensitivity and uncertainty analysis; consideration of local biomass availability
805 and biomass supply chains; variable part-load performance; investment planning; and multi-objective
806 optimization considering net present value (NPV) and 100-years global warming potential (GWP100a).

807 The methodology was applied in a simple case study where cellulosic ethanol production and upgraded
808 biogas production were considered for installation in an existing combined cycle combined heat and power
809 plant. The integration of ethanol production yielded more efficient results with respect to NPV and total
810 CO_2 emission impact than did the integration of combined ethanol and biomethane production. However,
811 the total CO_2 emission impact might conceivably have been reduced significantly for designs with
812 biomethane production if avoided CH_4 emissions from conventional use of manure had been considered.
813 The highest NPV and CO_2 emission impact was obtained for the reference combined heat and power plant,
814 illustrating that reducing CO_2 emissions come at a cost. The case study further demonstrated how
815 suboptimal designs would be obtained if systematic process integration was not considered, underlining
816 the importance of considering systematic process integration when developing smart energy systems in
817 general, and FMGs in particular.
818 The developed design methodology efficiently screens the solution space for promising FMG designs, and
819 is capable of assessing the importance of parameter uncertainties as well as estimating the likely
820 performance variation for the individual designs. Thus, the developed design methodology is useful for
821 conducting quick and reliable pre-feasibility analyses for the development of FMG concepts.

822 ## Acknowledgements

823 This research was supported by DONG Energy and the Innovation Foundation through the 4DH project. The
824 authors thank prof. Gürkan Sin, DTU Chemical Engineering, CAPEC-PROCESS, for fruitful discussions on
825 sensitivity and uncertainty analysis, and for allowing the use of his Matlab programs for conducting Morris
826 screening and Monte Carlo simulations. The authors also thank Ida Græsted Jensen, DTU Management
827 Engineering, Systems Analysis, for fruitful discussions on the modelling of biomass supply chains. Finally,
828 the authors would like to thank Bodil Diemer for linguistic comments and suggestions that greatly improved
829 the manuscript.

References

[1] G. Chicco and P. Mancarella, "Distributed multi-generation: A comprehensive view," *Renewable and Sustainable Energy Reviews*, vol. 13, no. 3. pp. 535–551, 2009.

[2] H. Song, F. Starfelt, L. Daianova, and J. Yan, "Influence of drying process on the biomass-based polygeneration system of bioethanol, power and heat," *Appl. Energy*, vol. 90, no. 1, pp. 32–37, 2012.

[3] H. Lund, A. N. Andersen, P. A. Østergaard, B. V. Mathiesen, and D. Connolly, "From electricity smart grids to smart energy systems - A market operation based approach and understanding," *Energy*, vol. 42, no. 1. pp. 96–102, 2012.

[4] M. Geidl, G. Koeppel, P. Favre-Perrod, B. Klöckl, G. Andersson, and K. Fröhlich, "Energy hubs for the future," *IEEE Power Energy Mag.*, vol. 5, no. 1, pp. 24–30, 2007.

[5] A. Coronas, S. S. Murthy, and J. Carles Bruno, "Editorial for the special issue of applied thermal engineering on polygeneration," *Appl. Therm. Eng.*, vol. 50, no. 2, pp. 1397–1398, 2013.

[6] H. Lund, F. Hvelplund, P. Østergaard, B. Möller, B. V. Mathiesen, D. Connolly, and A. N. Andersen, *Renewable Energy Systems*. 2014.

[7] H. Lund, *Renewable Energy Systems: The Choice and Modeling of 100% Renewable Solutions*. Academic Press publications, 2010.

[8] Z. Yuan and B. Chen, "Process synthesis for addressing the sustainable energy systems and environmental issues," *AIChE J.*, vol. 58, no. 11, pp. 3370–3389, 2012.

[9] L. M. Serra, M.-A. Lozano, J. Ramos, A. V. Ensinas, and S. A. Nebra, "Polygeneration and efficient use of natural resources," *Energy*, vol. 34, no. 5. pp. 575–586, 2009.

[10] W. Zhou, H. Yang, M. Rissanen, B. Nygren, and J. Yan, "Decrease of energy demand for bioethanol-based polygeneration system through case study," *Appl. Energy*, vol. 95, pp. 305–311, 2012.

[11] P. Ahmadi, I. Dincer, and M. a. Rosen, "Development and assessment of an integrated biomass-based multi-generation energy system," *Energy*, vol. 56, pp. 155–166, 2013.

[12] B. V. Mathiesen, H. Lund, D. Connolly, H. Wenzel, P. a. Østergaard, B. Möller, S. Nielsen, I. Ridjan, P.

Karnøe, K. Sperling, and F. K. Hvelplund, “Smart Energy Systems for coherent 100% renewable energy and transport solutions,” *Appl. Energy*, vol. 145, pp. 139–154, 2015.

[13] P. Mancarella, “MES (multi-energy systems): An overview of concepts and evaluation models,” *Energy*, vol. 65. pp. 1–17, 2014.

[14] C. Lythcke-Jørgensen, F. Haglind, and L. R. Clausen, “Exergy analysis of a combined heat and power plant with integrated lignocellulosic ethanol production,” *Energy Convers. Manag.*, vol. 85, pp. 817–827, 2014.

[15] M. Gassner and F. Maréchal, “Methodology for the optimal thermo-economic, multi-objective design of thermochemical fuel production from biomass,” *Comput. Chem. Eng.*, vol. 33, no. 3, pp. 769–781, 2009.

[16] L. Gerber, M. Gassner, and F. Maréchal, “Systematic integration of LCA in process systems design: Application to combined fuel and electricity production from lignocellulosic biomass,” *Comput. Chem. Eng.*, vol. 35, no. 7, pp. 1265–1280, 2011.

[17] L. Tock and F. Maréchal, “Co-production of hydrogen and electricity from lignocellulosic biomass: Process design and thermo-economic optimization,” *Energy*, vol. 45, no. 1, pp. 339–349, 2012.

[18] P. Liu, D. I. Gerogiorgis, and E. N. Pistikopoulos, “Modeling and optimization of polygeneration energy systems,” *Catal. Today*, vol. 127, no. 1–4, pp. 347–359, 2007.

[19] P. Liu, E. N. Pistikopoulos, and Z. Li, “A mixed-integer optimization approach for polygeneration energy systems design,” *Comput. Chem. Eng.*, vol. 33, no. 3, pp. 759–768, 2009.

[20] P. Liu and E. N. Pistikopoulos, “A Multi-Objective Optimization Approach to Polygeneration Energy Systems Design,” *AIChE J.*, vol. 56, no. 5, pp. 1218–1234, 2010.

[21] P. Liu, E. N. Pistikopoulos, and Z. Li, “Decomposition Based Stochastic Programming Approach for Polygeneration Energy Systems Design under Uncertainty,” *Ind. Eng. Chem. Res.*, vol. 49, no. 7, pp. 3295–3305, 2010.

[22] P. Liu, E. N. Pistikopoulos, and Z. Li, “Polygeneration Systems Engineering,” in *Process Systems*

Engineering, vol. 5, 2011, pp. 1–38.

[23] Y. Chen, T. A. Adams, and P. I. Barton, "Optimal design and operation of static energy polygeneration systems," *Ind. Eng. Chem. Res.*, vol. 50, no. 9, pp. 5099–5113, 2011.

[24] Y. Chen, T. A. Adams, and P. I. Barton, "Optimal design and operation of flexible energy polygeneration systems," *Ind. Eng. Chem. Res.*, vol. 50, no. 8, pp. 4553–4566, 2011.

[25] Y. Chen, X. Li, T. A. Adams II, and P. I. Barton, "Decomposition Strategy for the Global Optimization of Flexible Energy Polygeneration Systems," *AlChE*, vol. 58, no. 10, pp. 3080–3095, 2012.

[26] M. Tawarmalani and N. V. Sahinidis, "Global optimization of mixed-integer nonlinear programs: A theoretical and computational study," *Math. Program.*, vol. 99, no. 3, pp. 563–591, 2004.

[27] Y. Chen, "Optimal design and operation of energy polygeneration systems," 2013.

[28] C. Marnay, G. Venkataramanan, M. Stadler, A. S. Siddiqui, R. Firestone, and B. Chandran, "Optimal technology selection and operation of commercial-building microgrids," *IEEE Trans. Power Syst.*, vol. 23, no. 3, pp. 975–982, 2008.

[29] C. Rubio-Maya, J. Uche-Marcuello, A. Martínez-Gracia, and A. a. Bayod-Rújula, "Design optimization of a polygeneration plant fuelled by natural gas and renewable energy sources," *Appl. Energy*, vol. 88, no. 2, pp. 449–457, 2011.

[30] C. Rubio-Maya, J. Uche-Marcuello, and A. Martínez-Gracia, "Sequential optimization of a polygeneration plant," *Energy Convers. Manag.*, vol. 52, no. 8–9, pp. 2861–2869, 2011.

[31] A. Piacentino, C. Barbaro, F. Cardona, R. Gallea, and E. Cardona, "A comprehensive tool for efficient design and operation of polygeneration-based energy micro-grids serving a cluster of buildings. Part I: Description of the method," *Appl. Energy*, vol. 111, pp. 1204–1221, 2013.

[32] T. Capuder and P. Mancarella, "Techno-economic and environmental modelling and optimization of flexible distributed multi-generation options," *Energy*, vol. 71, pp. 516–533, 2014.

[33] T. Capuder and P. Mancarella, "Modelling and Assessment of the Techno-economic and Environmental Performance of Flexible Multi- Generation Systems," *18th Power Syst. Comput. Conf.*

905 *Wroclaw, Pol.*, 2014.
906 [34] E. Martínez Ceseña, T. Capuder, and P. Mancarella, “Flexible Distributed Multienergy Generation
907 System Expansion Planning Under Uncertainty,” *IEEE Trans. Smart Grid*, pp. 1–10, 2015.
908 [35] P. Voll, M. Lampe, G. Wrobel, and A. Bardow, “Superstructure-free synthesis and optimization of
909 distributed industrial energy supply systems,” *Energy*, vol. 45, no. 1, pp. 424–435, 2012.
910 [36] P. Voll, C. Klaffke, M. Hennen, and A. Bardow, “Automated superstructure-based synthesis and
911 optimization of distributed energy supply systems,” *Energy*, vol. 50, no. 1, pp. 374–388, 2013.
912 [37] B. Meyer, P. Voll, S. Kirschbaum, and A. Bardow, “MILP Optimization of Nonlinear Energy Systems by
913 Multivariate Piecewise-Affine Surrogate Modeling,” in *Proceedings of the 26th International*
914 *Conference on Efficiency, Cost, Optimization, Simulation and Environmental Impact of Energy*
915 *Systems*, 2013.
916 [38] P. Voll, M. Hennen, C. Klaffke, M. Lampe, and A. Bardow, “Exploring the near-optimal solution space
917 for the synthesis of distributed energy supply systems,” *Chem. Eng. Trans.*, vol. 35, pp. 277–282,
918 2013.
919 [39] P. Petruschke, G. Gasparovic, P. Voll, G. Krajačić, N. Duić, and A. Bardow, “A hybrid approach for the
920 efficient synthesis of renewable energy systems,” *Appl. Energy*, 2014.
921 [40] Z. Zhou, J. Zhang, P. Liu, Z. Li, M. C. Georgiadis, and E. N. Pistikopoulos, “A two-stage stochastic
922 programming model for the optimal design of distributed energy systems,” *Appl. Energy*, vol. 103,
923 pp. 135–144, 2013.
924 [41] M. Leung Pah Hang, E. Martinez-Hernandez, M. Leach, and A. Yang, “Engineering Design of Localised
925 Synergestic Production Systems,” in *25th European Symposium on Process Systems Engineering and*
926 *25th Symbposium on Computer Aided Process Engineering*, 2015.
927 [42] C. Lythcke-Jørgensen and F. Haglind, “Design optimization of a polygeneration plant producing
928 power , heat , and lignocellulosic ethanol,” *Energy Convers. Manag.*, vol. 91, pp. 353–366, 2015.
929 [43] F. Maréchal, C. Weber, and D. Favrat, “Multiobjective Design and Optimization of Urban Energy

930 Systems," in *Process Systems Engineering*, 2011, pp. 39–83.
931 [44] S. Fazlollahi and F. Maréchal, "Multi-objective, multi-period optimization of biomass conversion
932 technologies using evolutionary algorithms and mixed integer linear programming (MILP)," *Appl.*
933 *Therm. Eng.*, vol. 50, no. 2, pp. 1504–1513, 2013.
934 [45] S. Fazlollahi, G. Becker, and F. Maréchal, "Multi-objectives, multi-period optimization of district
935 energy systems: I. Selection of typical operating periods," *Comput. Chem. Eng.*, vol. 65, pp. 54–66,
936 2014.
937 [46] S. Fazlollahi, G. Becker, and F. Maréchal, "Multi-objectives, multi-period optimization of district
938 energy systems: II-Daily thermal storage," *Comput. Chem. Eng.*, vol. 71, pp. 648–662, 2014.
939 [47] S. Fazlollahi, G. Becker, and F. Maréchal, "Multi-objectives, multi-period optimization of district
940 energy systems: III. Distribution networks," *Comput. Chem. Eng.*, vol. 66, pp. 82–97, 2014.
941 [48] R. Bolliger, "Méthodologie de la synthèse des systèmes énergétiques industriels," 2010.
942 [49] C. Lythcke-Jørgensen, F. Haglind, A. V. Ensinas, and M. Münster, "A method for aggregating external
943 operating conditions in multi-generation plant optimization models," *Appl. Energy*, vol. under revi,
944 2015.
945 [50] M. W. Jack, "Scaling laws and technology development strategies for biorefineries and bioenergy
946 plants," *Bioresour. Technol.*, vol. 100, no. 24, pp. 6324–6330, 2009.
947 [51] R. Smith, *Chemical process design and integration*. Chister, West Sussex, England: John Wiley & Sons
948 Ltd, 2005.
949 [52] A. Boldrin, K. R. Baral, T. Fitamo, A. H. Vazifehkhoran, I. G. Jensen, I. Kjærgaard, Q. Van Nguyen, K.-A.
950 Lyng, L. Skovsgaard Nielsen, and J. M. Triolo, "A dynamic model for integrated optimization of Biogas
951 Production – A case study on Sugar Beet Biomass," *Energy*, vol. (in proces, 2015.
952 [53] S. Fazlollahi, P. Mandel, G. Becker, and F. Maréchal, "Methods for multi-objective investment and
953 operating optimization of complex energy systems," *Energy*, vol. 45, no. 1, pp. 12–22, 2012.
954 [54] R. L. Haupt and S. E. Haupt, *Practical Genetic Algorithms*. John Wiley & Sons, Inc., 2006.

[55] I. C. Kemp, *Pinch Analysis and Process Integration*. 2006.

[56] R. Turton, R. C. Bailie, W. B. Whiting, and J. a. Shaeiwitz, *Analysis, Synthesis, and Design of Chemical Processes*. 1998.

[57] M. D. Morris, "Factorial Sampling Plans for Preliminary Computational Experiments," *Technometrics*, vol. 33, no. 2, pp. 161–174, 1991.

[58] G. Sin, K. V. Gernaey, and A. E. Lantz, "Good modeling practice for PAT applications: Propagation of input uncertainty and sensitivity analysis," in *Biotechnology Progress*, 2009, vol. 25, no. 4, pp. 1043–1053.

[59] J. C. Helton and F. J. Davis, "Latin hypercube sampling and the propagation of uncertainty in analyses of complex systems," *Reliability Engineering and System Safety*, vol. 81, no. 1. pp. 23–69, 2003.

[60] M. D. McKay, R. J. Beckman, and W. J. Conover, "Comparison of three methods for selecting values of input variables in the analysis of output from a computer code," *Technometrics*, vol. 21, no. 2, pp. 239–245, 1979.

[61] J. Larsen, M. Ø. Haven, and L. Thirup, "Inbicon makes lignocellulosic ethanol a commercial reality," *Biomass and Bioenergy*, vol. 46, pp. 36–45, 2012.

[62] C. Lythcke-Jørgensen, M. Münster, A. V Ensinas, and F. Haglind, "Design optimization of flexible biomass-processing polygeneration plants using characteristic operation periods," in *World Renewable Energy Congress XIII*, 2014.

[63] "Silkeborg Forsyning." [Online]. Available: http://www.silkeborgforsyning.dk/. [Accessed: 13-Sep-2015].

[64] C. Lythcke-Jørgensen, "Modelling and Optimization of a Steam Co-generation Plant with Integrated Bio-ethanol Production," Technical University of Denmark, 2012.

[65] A. Evald, G. Hu, and M. T. Hansen, "Technology data for advanced bioenergy fuels," 2013.

[66] Energinet.dk and Danish Energy Agency, *Technology data for energy plants*, no. January 2014. 2012.

[67] M. Münster and P. Meibom, "Long-term affected energy production of waste to energy technologies

identified by use of energy system analysis," *Waste Manag.*, vol. 30, no. 12, pp. 2510–2519, 2010.

[68] Danish Energy Agency, "FORUDSÆTNINGER FOR SAMFUNDSØKONOMISKE ANALYSER PÅ ENERGIOMRÅDET," 2014.

[69] Ipcc, *2006 IPCC Guidelines for National Greenhouse Gas Inventories*, vol. 4. 2006.

[70] COWI, "FJERNVARMEANALYSE - BILAGSRAPPORT," 2014.

[71] Danish Energy Agency, "Danske nøgletal," 2015. [Online]. Available: http://www.ens.dk/info/tal-kort/statistik-nogletal/nogletal/danske-nogletal.

[72] J. Larsen, M. Øtergaard Petersen, L. Thirup, H. W. Li, and F. K. Iversen, "The IBUS process - Lignocellulosic bioethanol close to a commercial reality," *Chem. Eng. Technol.*, vol. 31, no. 5, pp. 765–772, 2008.

[73] E. Energianalyse, "Opdatering af samfundsøkonomiske brændselspriser - BIOMASSE," 2011.

[74] N. S. Bentsen, C. Felby, and K. H. Ipsen, "Energy balance of 2nd generation bioethanol production in Denmark," *Dong Energy R. Vet. Agric. Univ. Danish Cent. For. Landsc. Plan.*, 2006.

[75] T. A. Adams and J. H. Ghouse, "Polygeneration of fuels and chemicals," *Curr. Opin. Chem. Eng.*, vol. 10, pp. 87–93, 2015.

[76] E. Souleimanov and J. Kraus, "Turkey: An Important East-West Energy Hub," *Middle East Policy*, vol. 19, no. 2, pp. 157–168, 2012.

[77] K. Hemmes, J. L. Zachariah-Wolf, M. Geidl, and G. Andersson, "Towards multi-source multi-product energy systems," *Int. J. Hydrogen Energy*, vol. 32, no. 10–11, pp. 1332–1338, 2007.

Figure 1

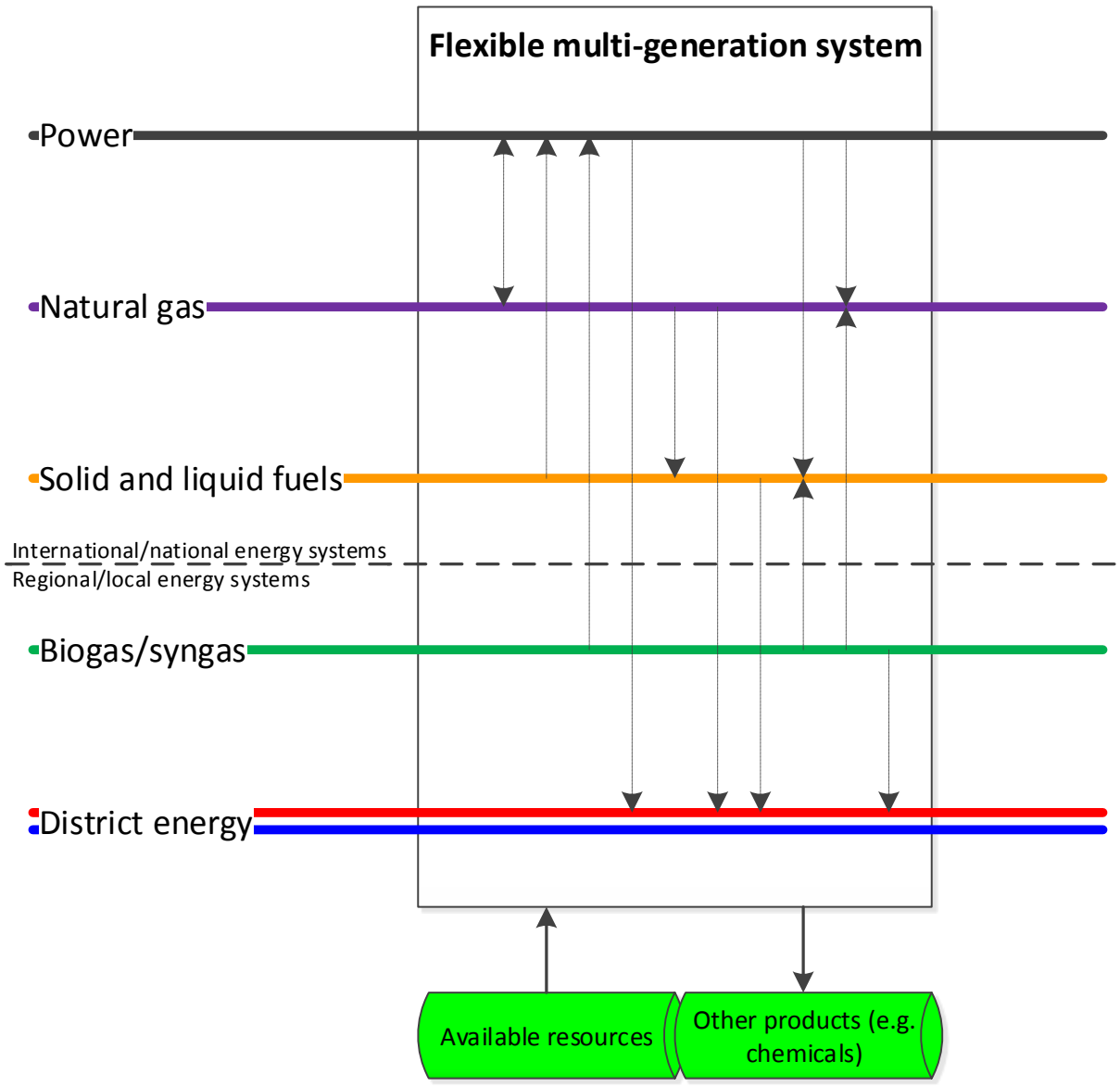

Figure 1: Conceptual sketch of a flexible multi-generation system. Dotted arrows indicate a range of technological pathways for linking the energy system layers.

Figure 2

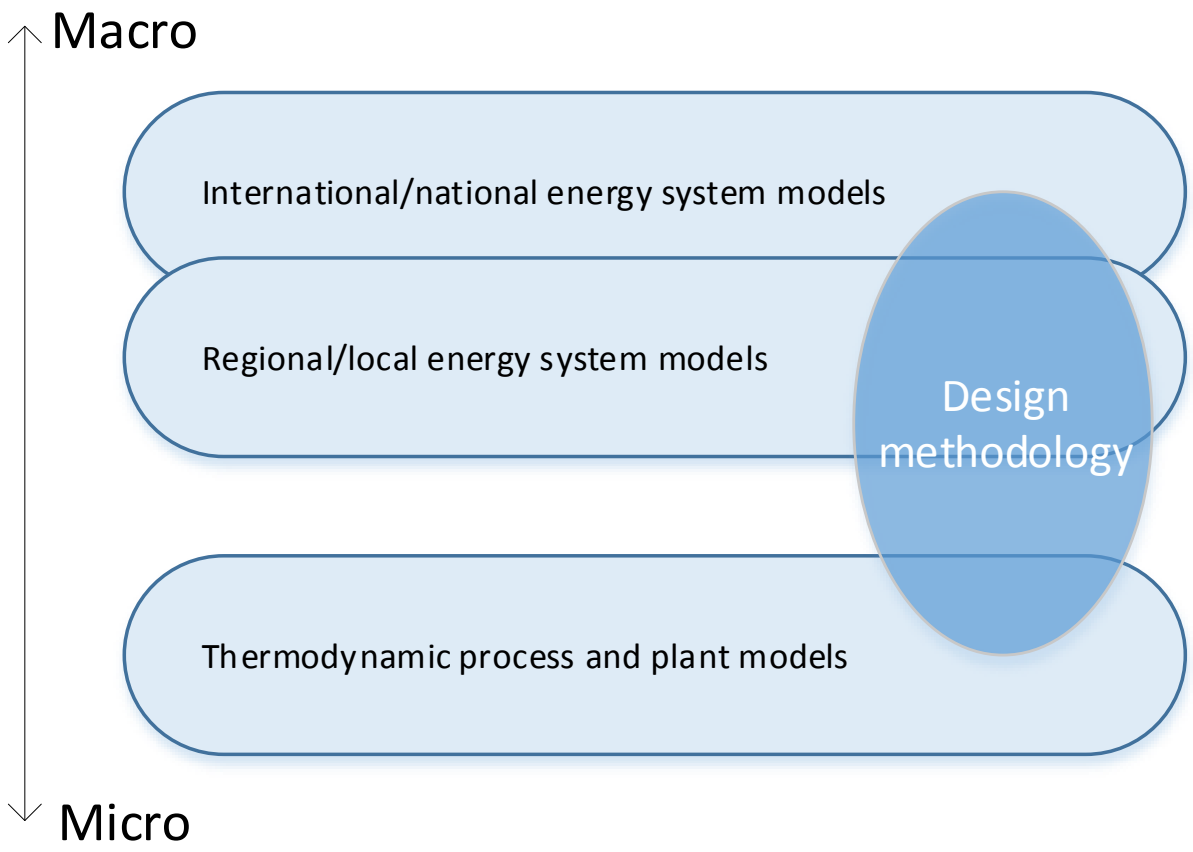

Figure 2: Visualization of how the design methodology interacts with models at various levels.

Figure 3

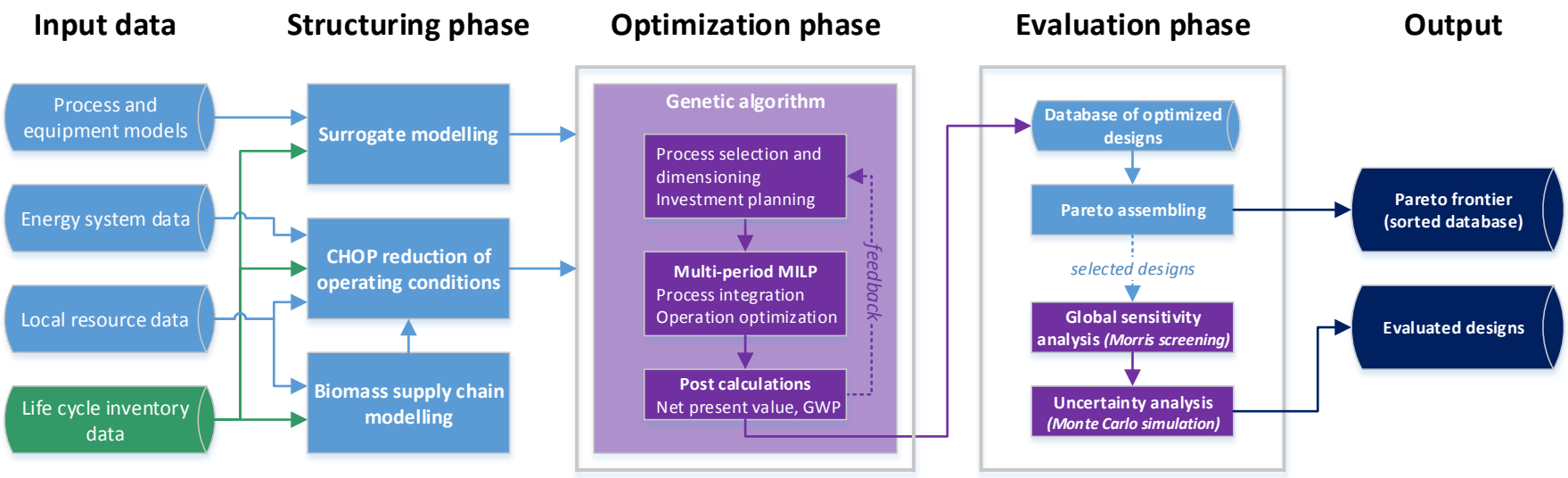

Figure 3: Design methodology structure.

Figure 4

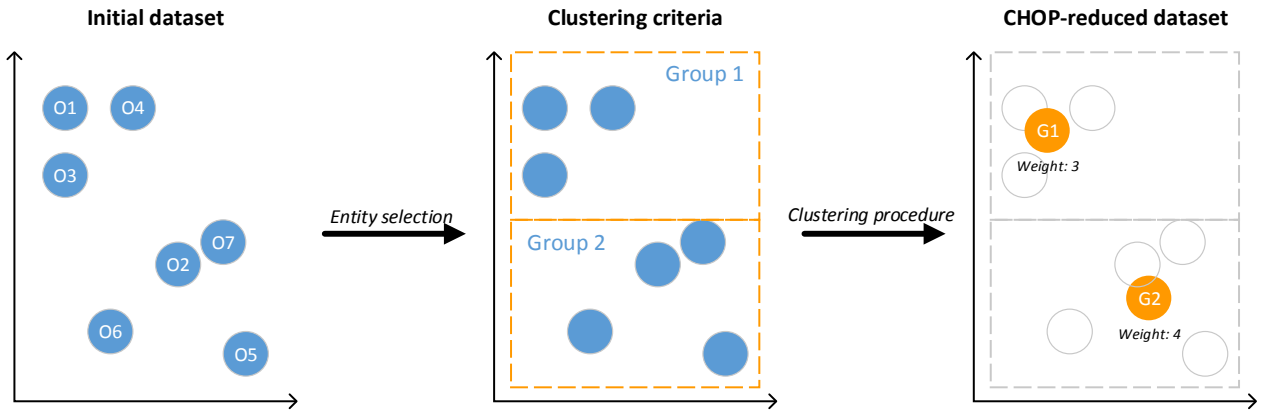

Figure 4: Principal sketch of the data aggregation principle applied in the CHOP method. Operating points O_j are clustered and merged into CHOP groups G_i with aggregated weight factors. Figure from [49].

Figure 5

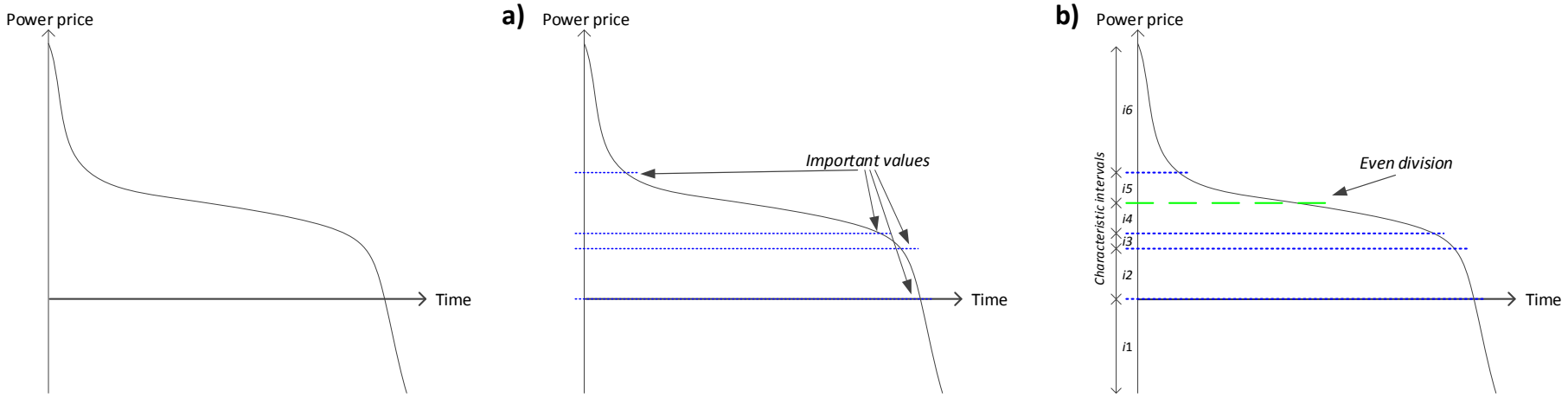

Figure 5: Illustrative example of the suggested two-step approach for defining characteristic intervals based on the cumulative parameter curve (left). Interval break points are set for a) Important values, and b) Even division. The characteristic intervals are indicated on the second axis in b). Figure from [49].

Figure 6

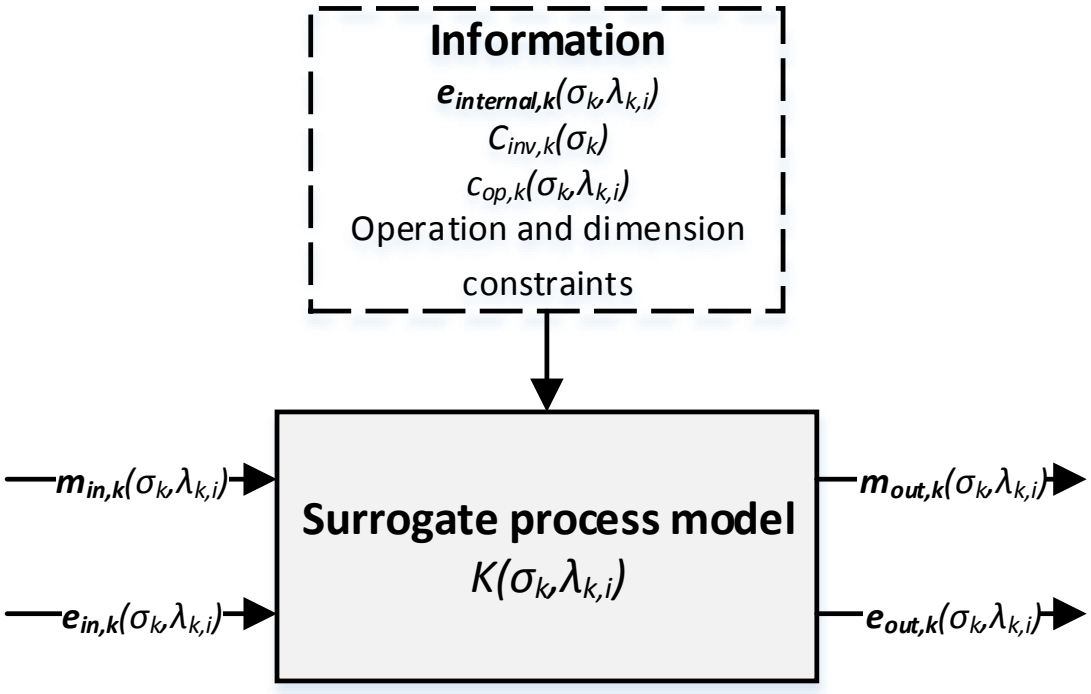

Figure 6: Generic illustration of a surrogate process model.

Figure 7

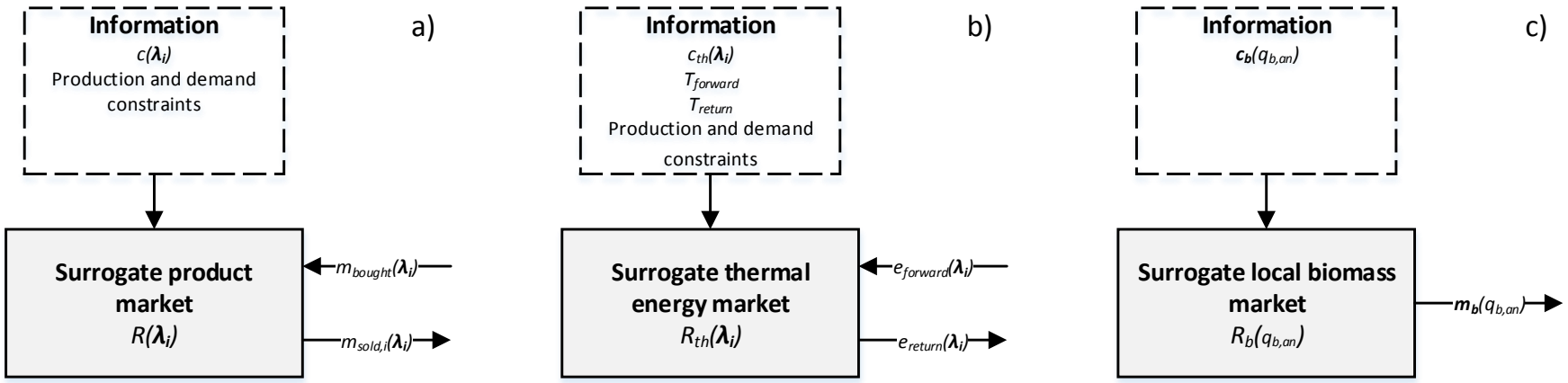

Figure 7: Generic illustration of a) a surrogate product or service market, b) a surrogate thermal energy market, and c) a surrogate local biomass market.

Figure 8

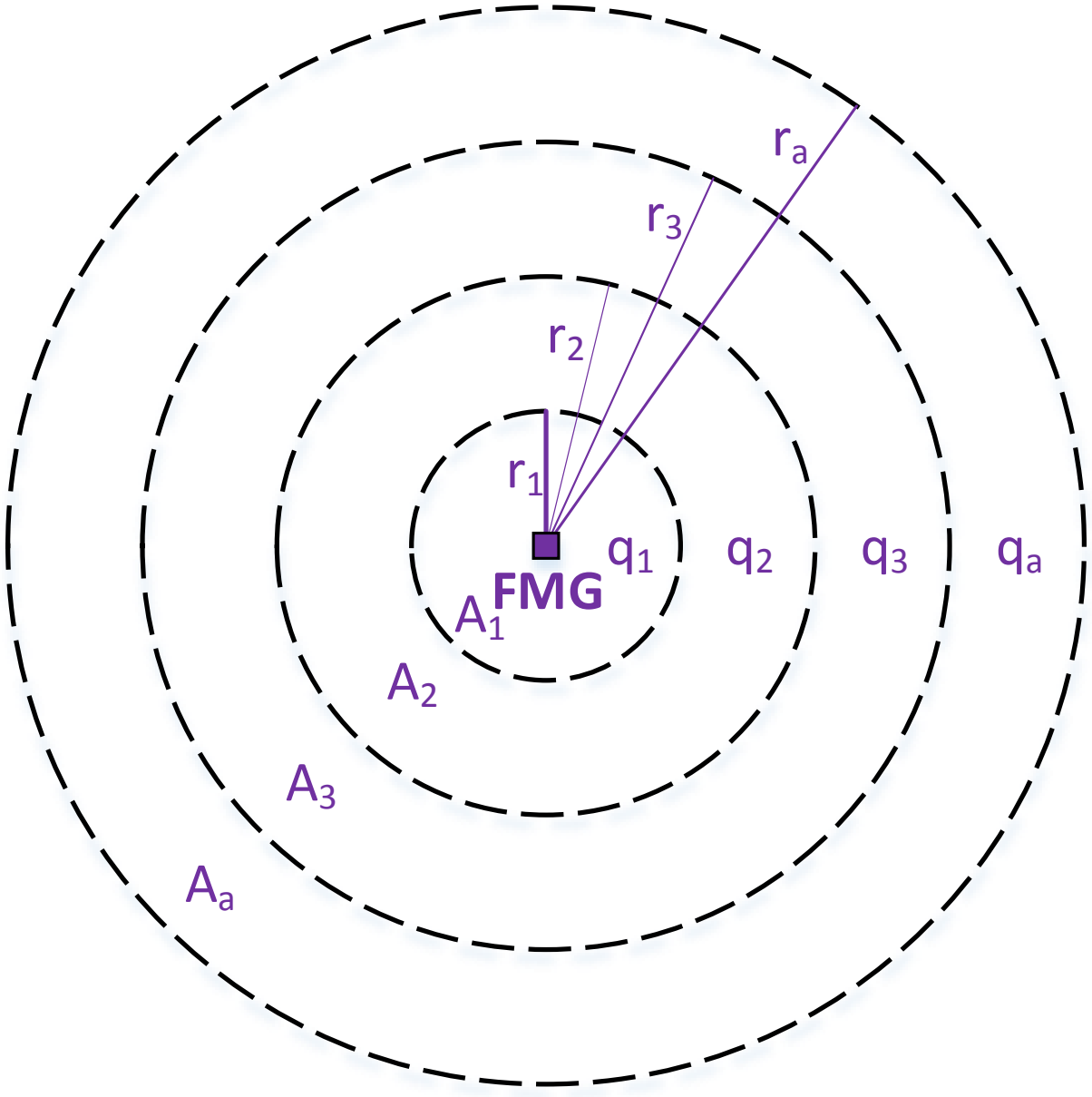

Figure 8: Applied land division around the FMG, with each circular area $\boldsymbol{A_a}$ being represented by an annual biomass production quantity $\boldsymbol{q_a}$, a minimum transportation distance $\boldsymbol{r_{a-1}}$ and a maximum transportation distance $\boldsymbol{r_a}$. The number of circular areas $\boldsymbol{A_a}$ is defined by the user.

Figure 9

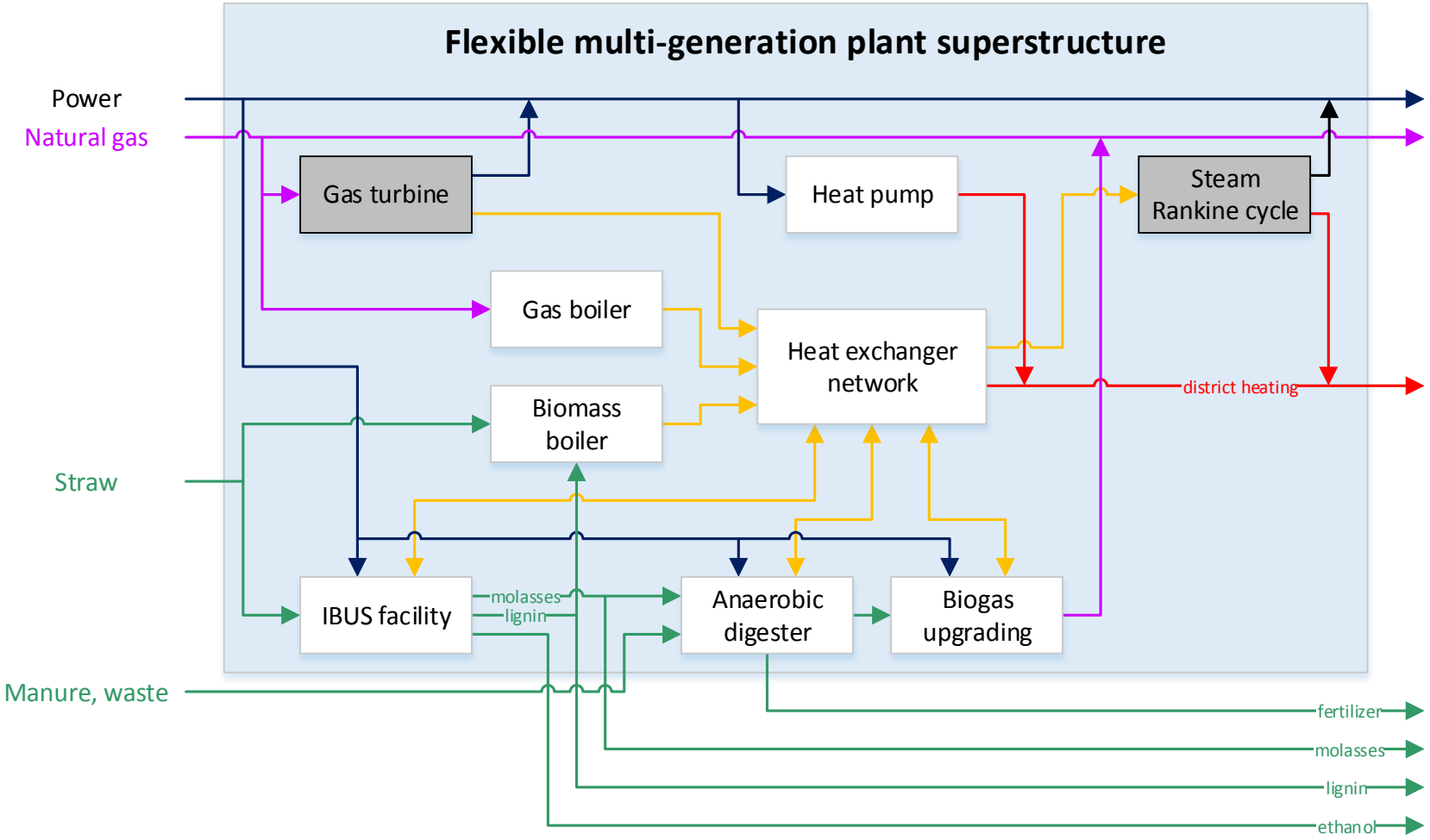

Figure 9: Superstructure of considered retrofit options for the existing combined cycle CHP. The gas turbine and steam Rankine cycle are grey as they are already installed.

Figure 10

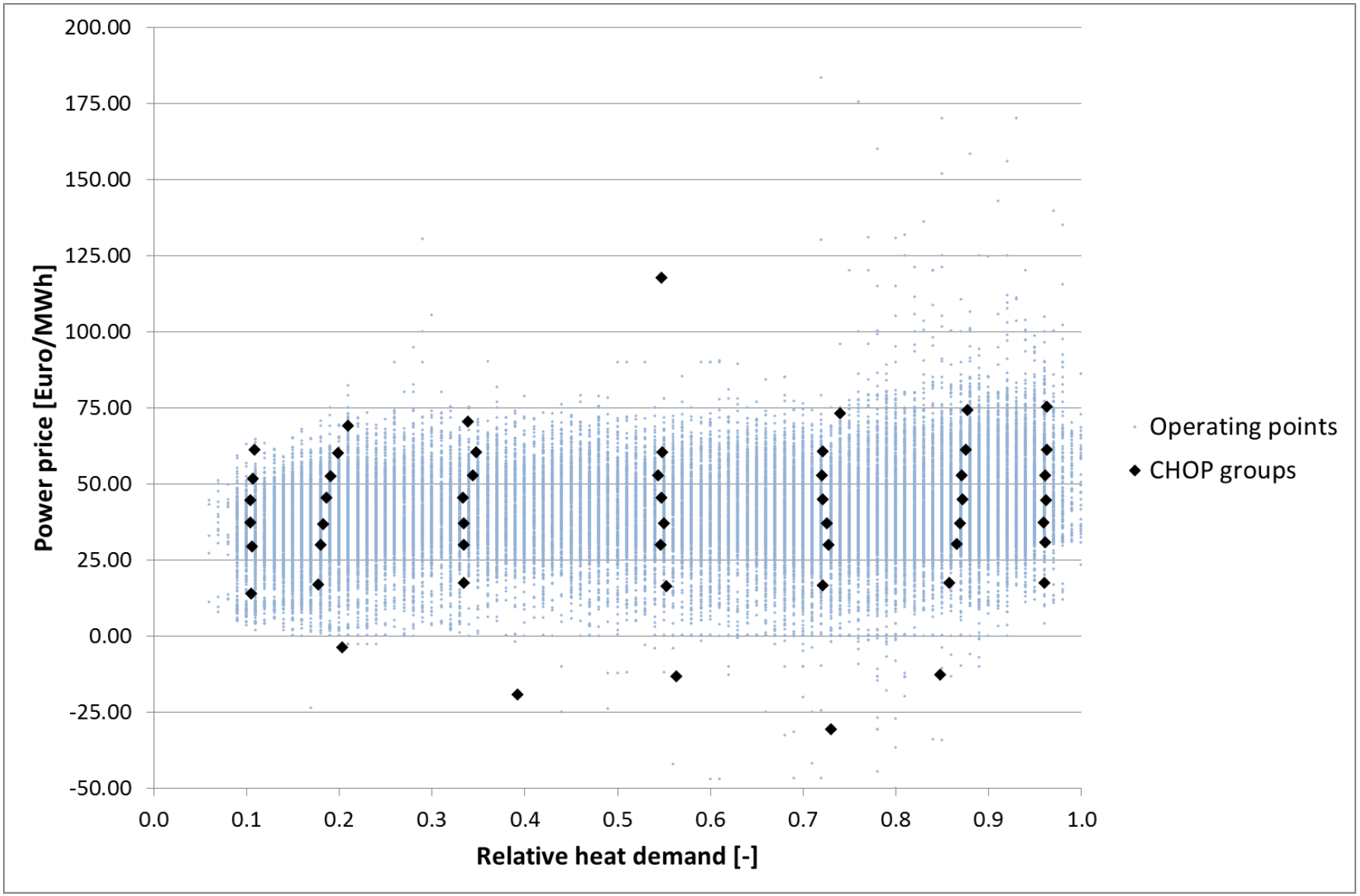

Figure 10: Scatter plot of reference operating points and CHOP groups with respect to power price and relative heat demand.

Figure 11

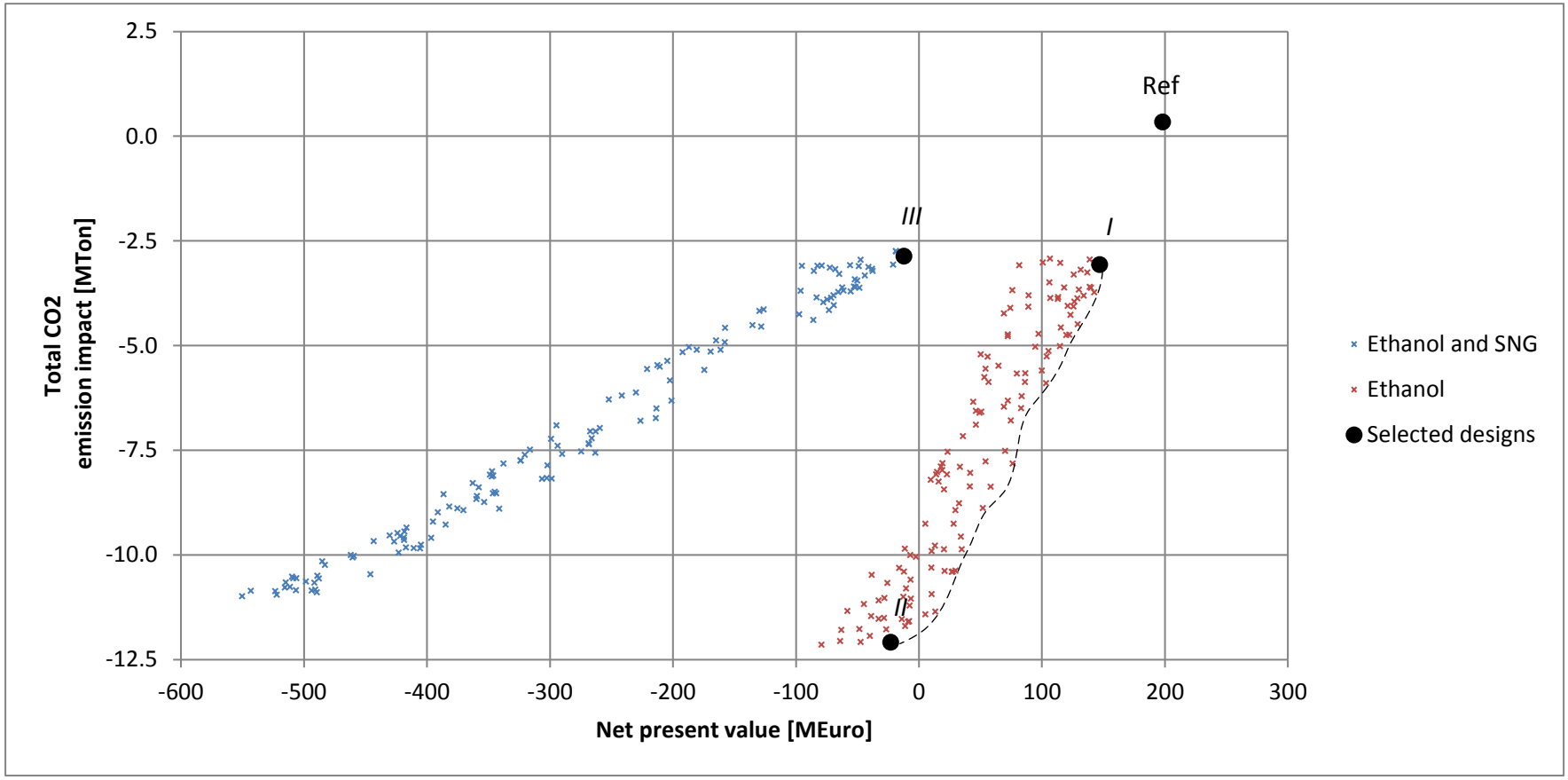

Figure 11: Scatter plot of optimized design solutions with respect to NPV and CO_2 emission impact. The designs are clustered according to type of biomass treatment installed. The dotted line crudely illustrates the identified Pareto curve. The designs marked '*I*', '*II*' and '*III*' are selected for further investigation. 'Ref' is the evaluated performance of the reference combined cycle CHP.

Figure 12

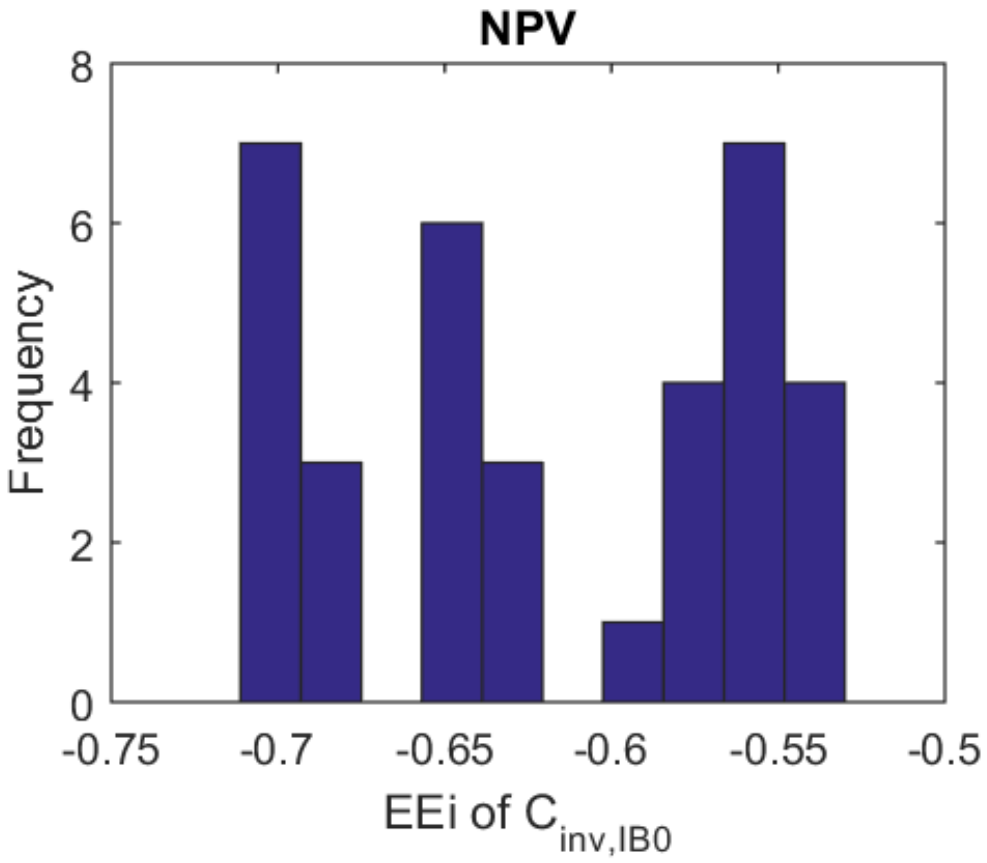

Figure 12: Histogram – elementary effect on NPV from reference ethanol facility Investment cost for design *I*.

Figure 13

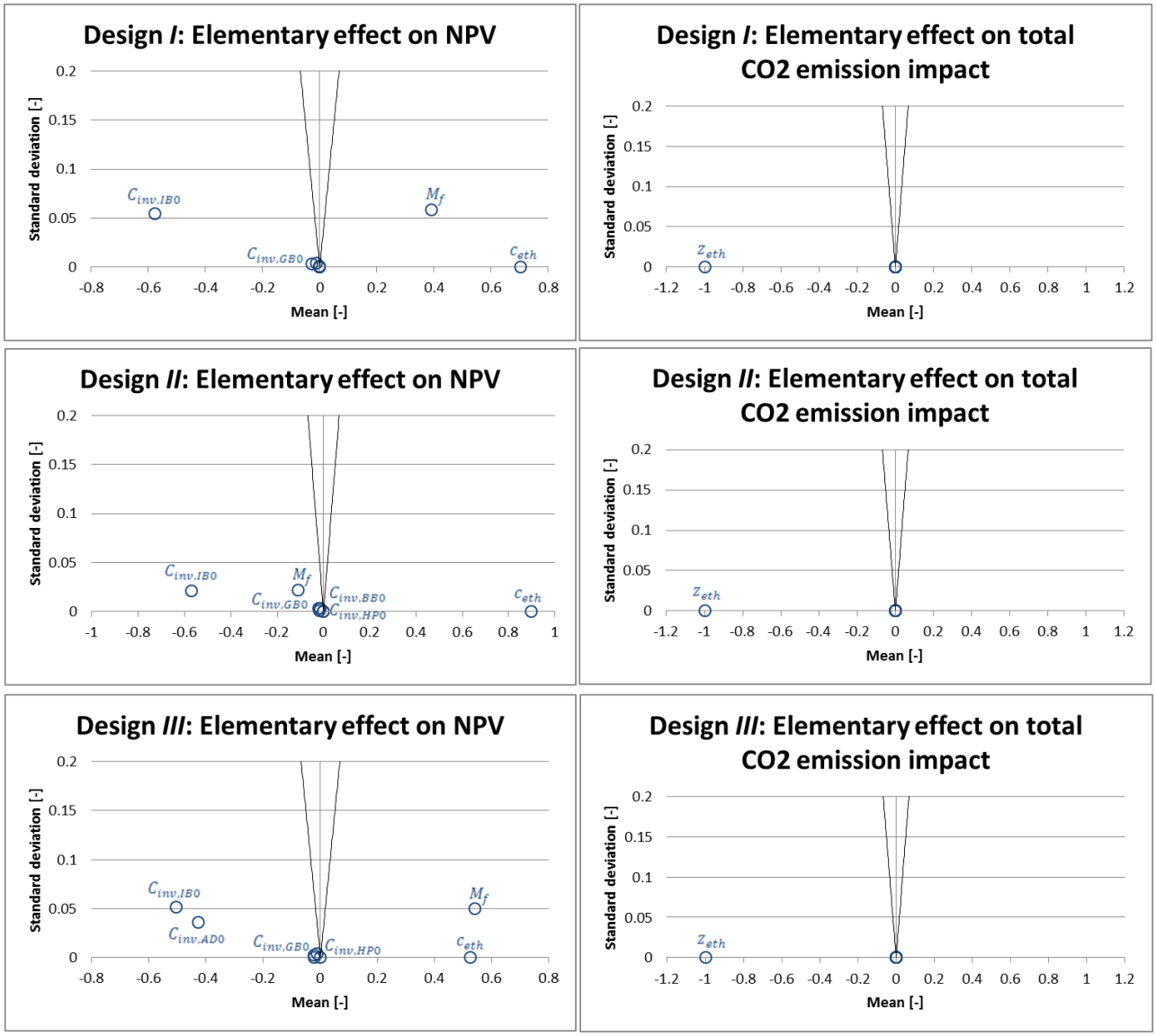

Figure 13: Means and standard deviations of sigma-scaled elementary effects on NPV (left) and total CO2 emission impact (right) from uncertain input parameters for designs *I* (top), *II* (middle), and *III* (bottom).

Figure 14

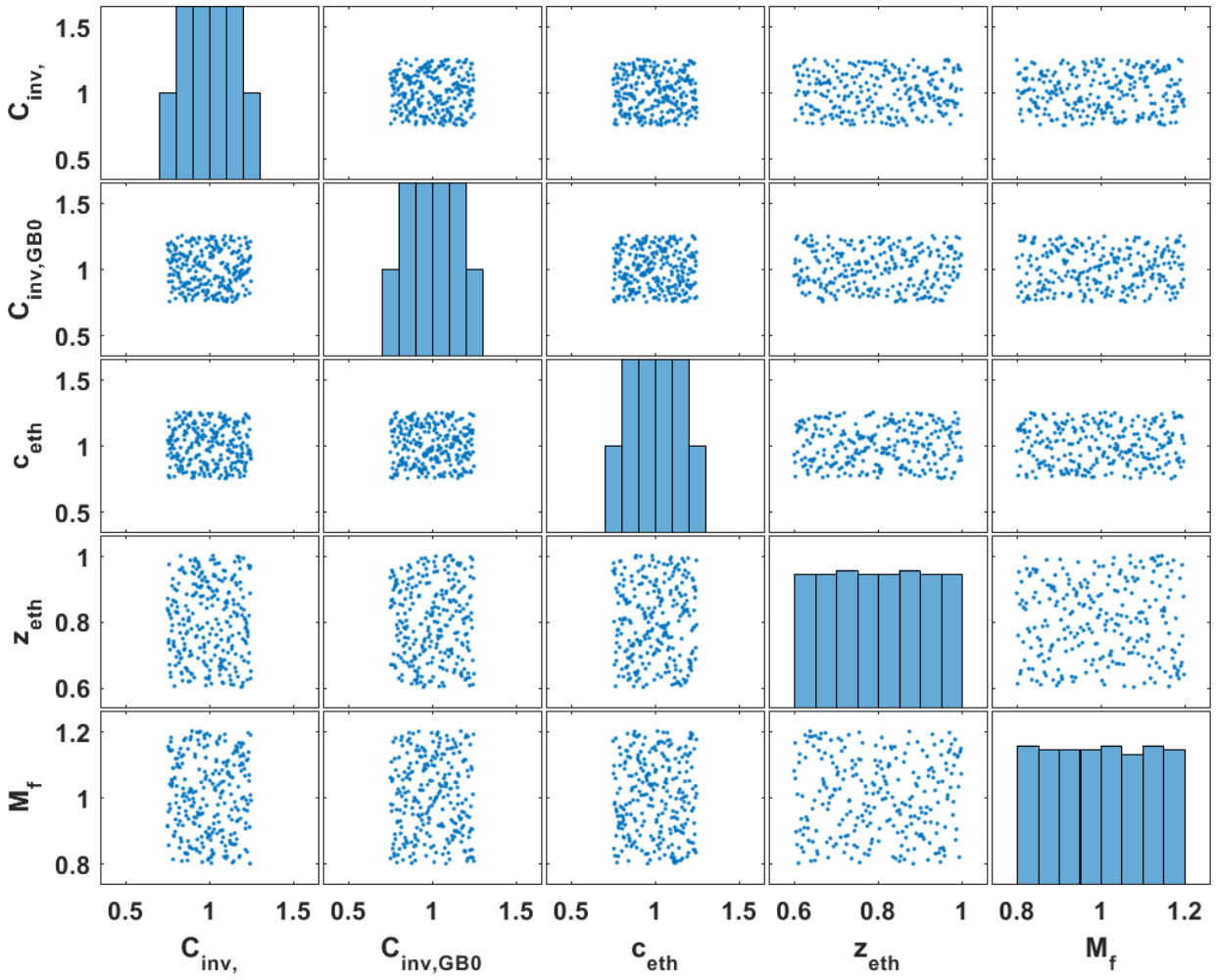

Figure 14: Example of Latin Hypercube Sampling – sample used for Monte Carlo simulations for design *I*.

Figure 15

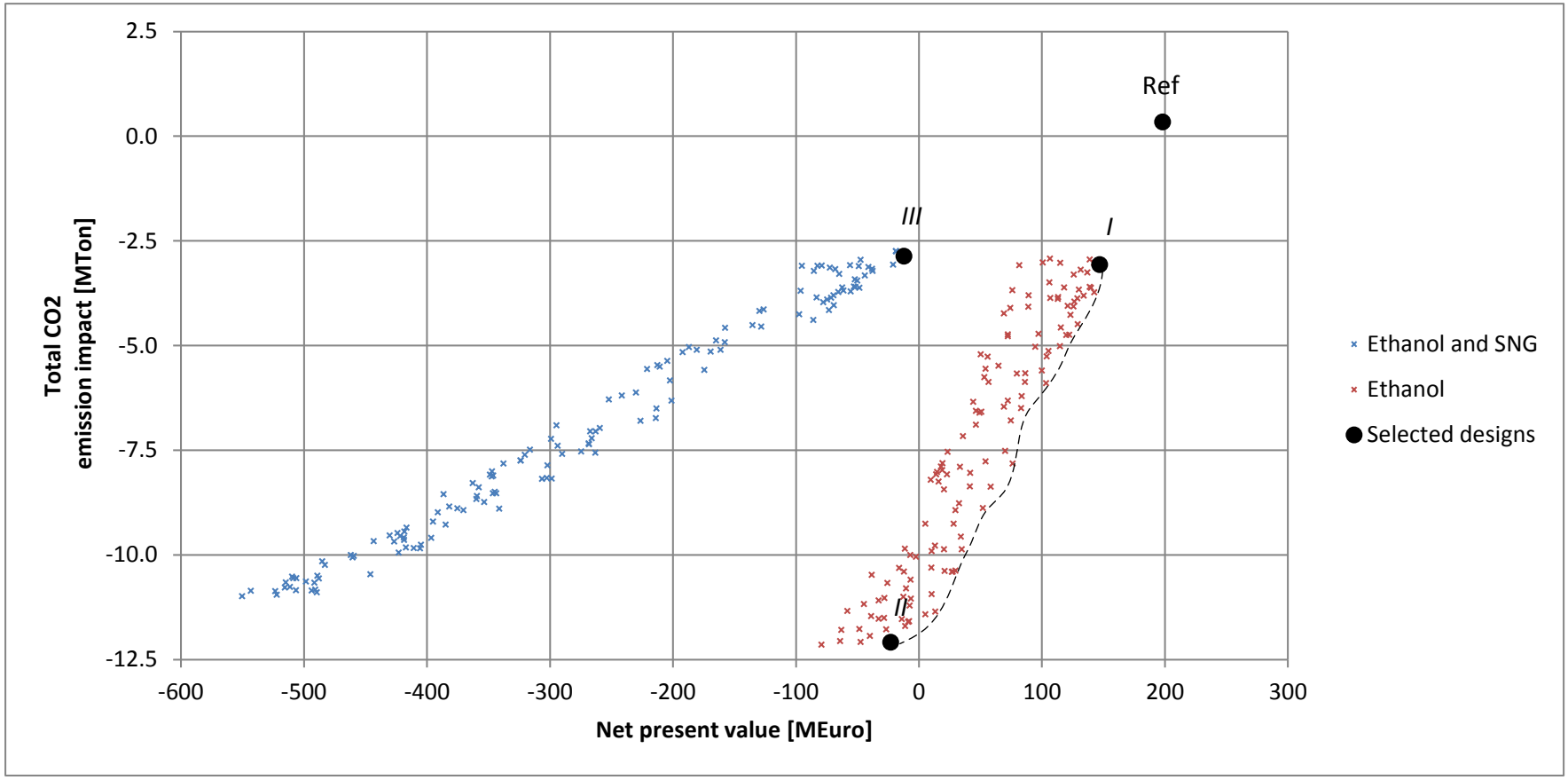

Figure 15: Scatter plot of optimized design solutions with respect to NPV and CO_2-emission impact, with performance variability indicated for each of the three selected designs. NPV performance intervals represent 10^{th} to 90^{th} percentiles of predicted performance, while CO_2 emission impact intervals represent 0^{th} to 90^{th} percentiles of predicted performance.

Figure 16

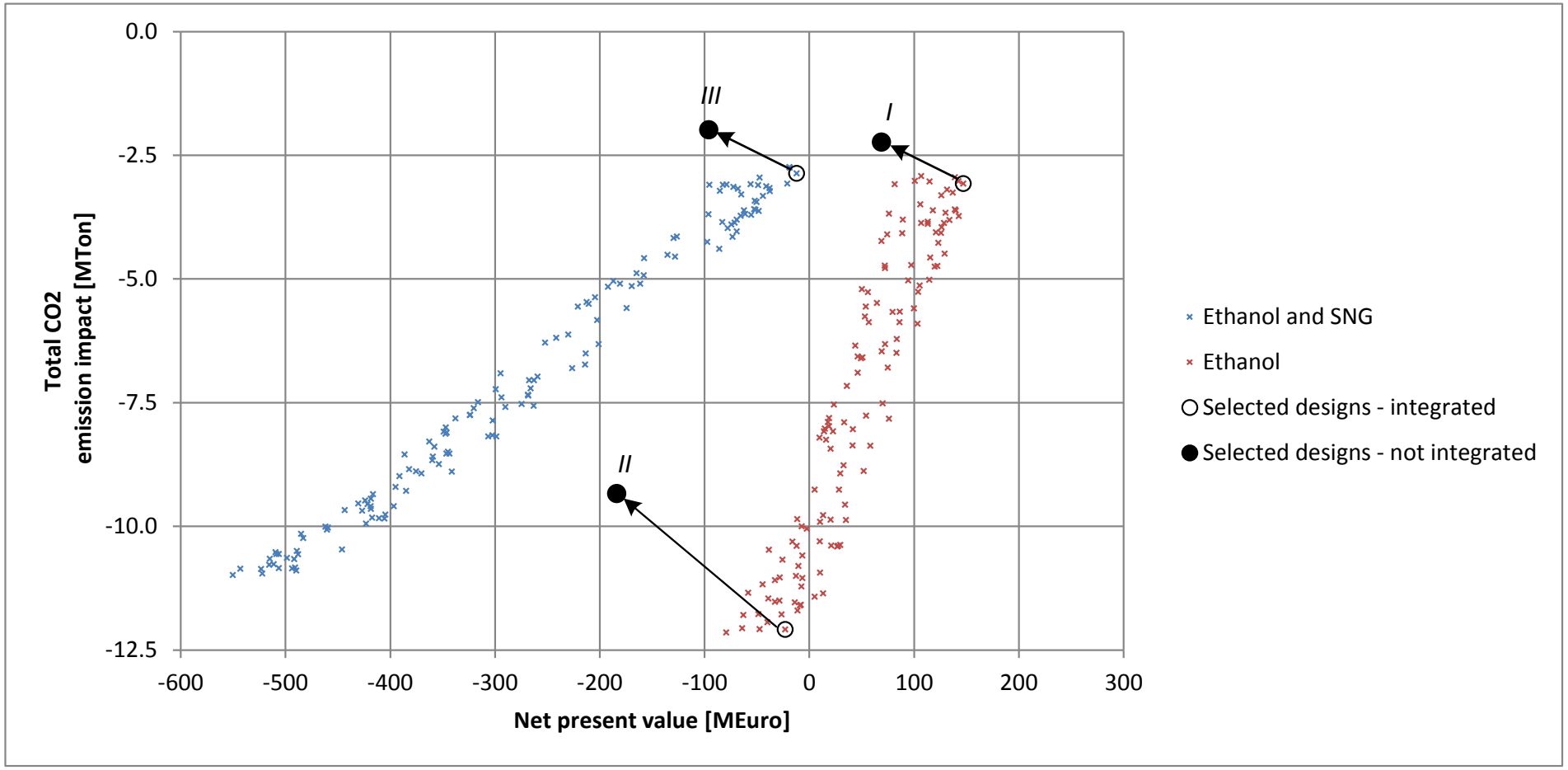

Figure 16: Performance of selected designs if systematic process integration had not been considered.

Table 1

Table 1: Data used for developing gas turbine and bottoming steam Rankine cycle surrogate models

Facility	Variable	Description	Value	Reference
Gas turbine (GT)	P_{GT100}	Nominal power capacity	85 MW	[63]
	$\dot{m}_{GT,gas100}$	Nominal gas consumption	216.25 MW	[63][a]
	$\dot{e}_{GT,off100}$	Nominal off-gas heat flow	105.3 MJ/s	[63][a]
	$T_{off,in}$	Off-gas temperature, before heat exchange	465°C	[63]
	$T_{off,out}$	Off-gas temperature after heat exchange	68°C	[63]
Rankine cycle (SR)	P_{SR100}	Nominal power capacity	23.3 MW	[63][a]
	Q_{SR100}	Nominal district heating generation	82.0 MJ/s	[63][a]
	$p_{SR,turbine,in}$	Turbine inlet pressure	15.5 bar	assumption
	$T_{SR,turbine,in}$	Turbine inlet temperature	450°C	assumption

[a]: Calculated based on operation data from [63]

Table 2

Table 2: Economic data on surrogate models

Model	Reference investment cost $C_{inv,k0}$	Reference operation and maintenance costs $c_{O\&M,k0}$	Reference dimension σ_{k0}
Gas turbine (GT)	-	2.50 Euro/MWh power [66]	-
Steam Rankine cycle (SR)	-	2.50 Euro/MWh power [66]	-
Ethanol facility (IB)	256.0 MEuro [65]	35.9 MEuro/year [65]	13.9 kg/s straw [65]
Biomethane facility (AD)	179.8 MEuro [65]	44.2 MEuro/year [65]	13.9 kg/s straw[b] [65]
Gas boiler (GB)	2.0 MEuro [66]	0.41 Euro/MWh heat [66]	20 MJ/s [66]
Biomass boiler (BB)	40 MEuro [66]	4.0 Euro/MWh heat [66]	50 MJ/s [66]
District heating heat pump (HP)	6.8 MEuro [66]	0.50 Euro/MWh heat [66]	10 MJ/s [66]

[b]: The biogas upgrading facility is dimensioned to process all C5-molasses from the reference ethanol facility if installed.

Table 3

Table 3: Thermal energy flow functions

Process	Flow-description	Notation	Type	Function [MJ/s]	T_{in}/T_{out}
Gas turbine (GT)	Off-gas heat flow	$\dot{e}_{GT,off}$	Hot	$1.053 \cdot \lambda_{GT}$	465°C /68°C
Steam Rankine cycle (SR)	Water heating	$\dot{e}_{SR,c1}$	Cold	$0.200 \cdot \lambda_{SR}$	120°C /200°C
	Water evaporation	$\dot{e}_{SR,c2}$	Cold	$0.653 \cdot \lambda_{SR}$	200°C /200°C
	Steam superheating	$\dot{e}_{SR,c3}$	Cold	$0.200 \cdot \lambda_{SR}$	200°C /450°C
	Condensation	$\dot{e}_{SR,h}$	Hot	$0.820 \cdot \lambda_{SR}$	120°C /120°C
Ethanol facility (IB)	Steam generator, water heating	$\dot{e}_{IB,sg1}$	Cold	$1.501 \cdot \sigma_{IB}$	15°C /192°C
	Steam generator, evaporation	$\dot{e}_{IB,sg2}$	Cold	$3.945 \cdot \sigma_{IB}$	192°C /192°C
	Steam generator, superheating	$\dot{e}_{IB,sg3}$	Cold	$0.019 \cdot \sigma_{IB}$	192°C /195°C
	Pretreatment, cooling 1	$\dot{e}_{IB,pr1}$	Hot	$0.341 \cdot \sigma_{IB}$	190°C /100°C
	Pretreatment, cooling 2	$\dot{e}_{IB,pr2}$	Hot	$4.287 \cdot \sigma_{IB}$	100°C /100°C
	Pretreatment, cooling 3	$\dot{e}_{IB,pr3}$	Hot	$0.092 \cdot \sigma_{IB}$	100°C /80°C
	Pretreatment, cooling 4	$\dot{e}_{IB,pr4}$	Hot	$0.247 \cdot \sigma_{IB}$	100°C /50°C
	Liquefaction cooling	$\dot{e}_{IB,lq}$	Hot	$0.060 \cdot \sigma_{IB}$	50°C /33°C
	Distillation, heating 1	$\dot{e}_{IB,dsh1}$	Cold	$1.631 \cdot \sigma_{IB}$	100°C /100°C
	Distillation, heating 2	$\dot{e}_{IB,dsh2}$	Cold	$0.021 \cdot \sigma_{IB}$	33°C /37°C
	Distillation, cooling 1	$\dot{e}_{IB,dsc1}$	Cold	$1.044 \cdot \sigma_{IB}$	68°C /68°C
	Distillation, cooling 2	$\dot{e}_{IB,dsc2}$	Cold	$0.807 \cdot \sigma_{IB}$	100°C /30°C
Biomethane facility (AD)	Anaerobic digester, heating	$\dot{e}_{AD,h}$	Cold	$0.249 \cdot \omega_{AD}\sigma_{IB}$	55°C /55°C
	Gas upgrading heat loss	$\dot{e}_{AD,l}$	Hot	$0.767 \cdot \omega_{AD}\sigma_{IB}$	100°C /30°C
Gas boiler (GB)	Gas boiler off-gas	$\dot{e}_{GB}$	Hot	$\lambda_{GB}\sigma_{GB}$	465°C /68°C
Biomass boiler (BB)	Biomass boiler off-gas	$\dot{e}_{GB}$	Hot	$\lambda_{BB}\sigma_{BB}$	465°C /68°C
District heating heat pump (HP)	Heat pump heat delivery	$\dot{e}_{HP}$	Hot	$\lambda_{HP}\sigma_{HP}$	90°C /90°C
District heating demand (DH)	Heating of return flow	$\dot{e}_{DH}$	Cold	λ_{DH}	40°C /80°C

Table 4

Table 4: Power flow functions

Process	Flow-description	Notation	Function [MW]
Gas turbine (GT)	GT power generation	$\dot{m}_{GT,el}$	$0.85 \cdot \lambda_{GT}$
Steam Rankine cycle (SR)	SR power generation	$\dot{m}_{SR,el}$	$0.233 \cdot \lambda_{SR}$
Ethanol facility (IB)	IB power consumption	$\dot{m}_{IB,el}$	$-0.583 \cdot \sigma_{IB}$
Combined biogas facility (AD)	AD power consumption	$\dot{m}_{AD,el}$	$-2.048 \cdot \omega_{AD}\sigma_{IB}$
District heating heat pump (HP)	HP power consumption	$\dot{m}_{HP,el}$	$-0.357 \cdot \sigma_{HP}$
Power market	Power market exchange	$\dot{m}_{R,el}$	

Table 5

Table 5: Straw flow functions

Process	Flow-description	Notation	Function [MJ/s]
Ethanol facility (IB)	Ethanol straw consumption	$\dot{m}_{IB,straw}$	$-15.1 \cdot \sigma_{IB}$
Biomass boiler (BB)	Biomass boiler straw consumption	$\dot{m}_{BB,straw}$	$-1.031 \cdot \sigma_{IB}$
Straw market	Straw import	$\dot{m}_{R,el}$	

Table 6

Table 6: Solid biofuel flow functions

Process	Flow-description	Notation	Function [MJ/s]
Ethanol facility (IB)	Ethanol solid biofuel production	$\dot{m}_{IB,biofuel}$	$7.1 \cdot \sigma_{IB}$
Biomass boiler (BB)	Biomass boiler biofuel consumption	$\dot{m}_{BB,biofuel}$	$-1.031 \cdot \sigma_{BB}\lambda_{BB,biofuel}$
Solid biofuel market	Solid biofuel export	$\dot{m}_{R,biofuel}$	

Table 7

Table 7: C5 residues flow functions

Process	Flow-description	Notation	Function [MJ/s]
Ethanol facility (IB)	Ethanol molasses production	$\dot{m}_{IB,mol}$	$3.9 \cdot \sigma_{IB}$
Combined biogas facility (AD)	Anaerobic digester molasses consumption	$\dot{m}_{AD,mol}$	$-3.9 \cdot \omega_{AD}\sigma_{IB}$
C5 residues market	C5 residues export	$\dot{m}_{R,mol}$	

Table 8

Table 8: Natural gas flow functions

Process	Flow-description	Notation	Function [MJ/s]
Gas turbine (GT)	Gas turbine gas consumption	$\dot{m}_{GT,gas}$	$-2.165 \cdot \lambda_{GT}$
Combined biogas facility (AD)	Upgraded biogas production	$\dot{m}_{AD,gas}$	$3.108 \cdot \omega_{AD}\sigma_{IB}$
Gas boiler (GB)	Gas boiler consumption	$\dot{m}_{GB,gas}$	$-1.031 \cdot \sigma_{GB}\lambda_{GB}$
Natural gas market	Natural gas market exchange	$\dot{m}_{R,gas}$	

Table 9

Table 9: Interval break points in the CHOP-reduced dataset.

Interval break point	1	2	3	4	5	6	7
Power price [Euro/MWh]	0.00	25.00	33.00	41.00	49.00	57.00	65.00
Relative heat demand [-]	0.125	0.25	0.45	0.65	0.80	0.95	-

Table 10

Table 10: Duration of the defined CHOP groups in hours. Note that the duration is multiplied by six to represent the 30-year lifetime of the facility rather than the 5-year period that the historical values are taken from.

CHOP group duration [h] Heat interval \ power interval	1	2	3	4	5	6	7	8
1	0	1,926	2,136	1,836	1,452	330	60	0
2	66	7,068	13,188	12,666	11,232	5,880	1,170	330
3	54	3,690	8,298	10,038	8,400	6,900	2,442	1,068
4	132	4,302	8,412	9,600	8,898	6,510	3,108	1,188
5	432	5,682	10,944	12,978	9,390	6,834	3,462	1,638
6	180	3,492	11,718	15,846	10,656	7,806	5,388	5,418
7	0	276	1,134	2,190	1,602	1,170	1,062	1,266

Table 11

Table 11: Relative heat demand of the defined CHOP groups

Relative heat demand [-] Heat interval \ power interval	1	2	3	4	5	6	7	8
1	-	0.105	0.106	0.105	0.105	0.107	0.109	-
2	0.204	0.178	0.180	0.182	0.186	0.191	0.199	0.210
3	0.392	0.334	0.335	0.334	0.334	0.344	0.348	0.339
4	0.563	0.553	0.546	0.550	0.547	0.544	0.549	0.547
5	0.731	0.721	0.727	0.726	0.721	0.720	0.721	0.740
6	0.848	0.858	0.866	0.870	0.872	0.871	0.876	0.878
7	-	0.961	0.961	0.960	0.962	0.961	0.963	0.963

Table 12

Table 12: Power price of the defined CHOP groups

Power price [€/MWh] Heat interval \ power interval	1	2	3	4	5	6	7	8
1	-	13.91	29.32	37.20	44.49	51.62	61.11	-
2	-3.92	16.86	29.73	36.73	45.20	52.51	60.05	69.02
3	-19.24	17.43	29.80	36.80	45.40	52.64	60.23	70.32
4	-13.46	16.22	29.77	36.83	45.20	52.59	60.34	117.54
5	-30.81	16.58	29.75	36.82	44.74	52.63	60.39	72.97
6	-12.90	17.36	30.03	36.98	44.76	52.59	61.08	74.10
7	-	17.20	30.56	37.11	44.58	52.75	60.95	75.08

Table 13

Table 13: Economic data on, and CO_2 emission impacts of, consumed and sold products

Products	Price [Euro/GJ]	CO2 standard emission factor [kg/GJ]	
		Consumed	Sold
Straw	5.70 [68]	0.00	-
Natural gas	6.24 [68]	56.1	-56.1[c] [69]
District heating	12.08[d] [70]	-	-33.0[e] [71]
Molasses (C5 residues)	5.38 [72]	-	0.00[f] [69]
Solid biofuel (lignin)	8.71 [68]	0.00	-101.1[g] [69]
Ethanol	16.05[h] [68]	-	-69.2[h] [69]
Power	[defined in CHOP]	0.413/0[i] [71]	-0.413/0[i] [71]

[c]: Sold natural gas (bio-methane) is assumed to replace natural gas in the grid.
[d]: Reference heat-to-grid selling price in 2020 for natural gas-based combined cycle power plants in western Denmark.
[e]: Average CO2 emission for district heating in Denmark.
[f]: For simplicity, no avoided CO_2 emission is associated with sold molasses. In reality, molasses may be sold as animal feed, thereby potentially replacing imported soy beans or similar, thus reducing CO_2 emissions.
[g]: The solid biofuel, from which most of the alkaline metals have been removed, is assumed to replace coal.
[h]: Ethanol is assumed to be sold as, and replace, gasoline.
[i]: Marginal power generation CO_2 emission is set equal to the average CO_2 emission from power generation in Denmark, apart from periods with negative power prices where the marginal CO_2 emission is set to zero to represent wind turbine power generation.

Table 14

Table 14: Biomass supply chain model

Area	Radius	Annual yield $q_{b,an}$ [ton]	Fixed logistics costs $c_{b,0}$ [Euro/GJ]	Transport costs $c_{b,tr}$ [Euro/GJ]	Marginal straw cost c_b [Euro/GJ]
A_1	10km	26,269	0.005	0	5.709
A_2	30km	210,154	0.005	0.215	5.924
A_3	50km	420,308	0.005	0.397	6.102

Table 15

Table 15: Design optimization variables and constraints

Design variable	Description	Lower bound	Upper bound
σ_{IB}	Ethanol facility dimension, in kg/s straw processed	5 kg straw/s	20 kg straw/s[j]
ω_{AD}	Installation of a combined biogas facility, decision	Integer decision $\{0,1\}$	
σ_{BB}	Biomass boiler dimension, in MJ/s heat delivered	0 MJ/s	100 MJ/s
σ_{HP}	District heating heat pump dimension, in MJ/s heat delivered	0 MJ/s	50 MJ/s

[j]: Equal to the maximum annual production of straw within a 50km radius of the plant under the assumptions in section 3.1.3.

Table 16

Table 16: Operation optimization variables and constraints

Operation variable	Description	Lower bound	Upper bound
$\boldsymbol{\nu_{GT}}$	Gas turbine operated	Integer decision $\{0,1\}$	
$\boldsymbol{\lambda_{GT}}$	Gas turbine load	0.20	1.00
$\boldsymbol{\nu_{GT}}$	Steam Rankine cycle operated	Integer decision $\{0,1\}$	
$\boldsymbol{\lambda_{SR}}$	Steam Rankine cycle load	0.40	1.00
$\boldsymbol{\lambda_{GB}}$	Gas boiler load	0.00	1.00
$\boldsymbol{\lambda_{BB}}$	Biomass boiler load	0.00	1.00
$\boldsymbol{\lambda_{HP}}$	Heat pump load	0.00	1.00

Table 17

Table 17: Uncertain parameters and their distributions

Parameter	Description	Distribution	Reference value	Lower bound	Upper bound
$C_{inv,IB0}$	Investment cost, reference ethanol facility	Uniform	256.0 MEuro	192.0 MEuro	320.0 MEuro
$C_{inv,AD0}$	Investment cost, reference combined biogas facility	Uniform	199.8 MEuro	149.9 MEuro	249.8 MEuro
$C_{inv,GB0}$	Investment cost, reference gas boiler	Uniform	2.0 MEuro	1.5 MEuro	2.5 MEuro
$C_{inv,BB0}$	Investment cost, reference biomass boiler	Uniform	40.0 MEuro	30.0 MEuro	50.0 MEuro
$C_{inv,HP0}$	Investment cost, reference district heating heat pump	Uniform	6.8 MEuro	5.1 MEuro	8.5 MEuro
c_{eth}	Ethanol price	Uniform	5.70 Euro/GJ	4.28 Euro/GJ	7.13 Euro/GJ
z_{eth}	Ethanol displaced CO_2 emission	Uniform	-69.2 kg/GJ	-41.5 kg/GJ	-69.2 kg/GJ
M_f	Investment scaling constant	Uniform	0.75	0.6	0.9

Table 18

Table 18: Characteristics of the selected designs

Design	NPV [MEuro]	CO_2-emission impact [MTon]	σ_{IB} [kg/s]	ν_{AD} [-]	σ_{GB} [MJ/s]	σ_{BB} [MJ/s]	σ_{HP} [MJ/s]	C_{HEN} [MEuro]
Ref	198.2	0.34	0.0	0	0.0	0.0	0.0	0
I	147.0	-3.07	5.2	0	80.1	1.1	0.3	4.83
II	-22.9	-12.09	19.6	0	143.8	11.1	19.8	7.51
III	-12.1	-2.87	5.3	1	70.0	1.3	9.0	4.98

Table 19

Table 19: Uncertain input parameters considered in Monte Carlo simulations for each of the three selected designs

Design	$C_{inv,IB0}$	$C_{inv,AD0}$	$C_{inv,GB0}$	$C_{inv,BB0}$	$C_{inv,HP0}$	c_{eth}	z_{eth}	M_f
I	X		X			X	X	X
II	X		X	X	X	X	X	X
III	X	X	X		X	X	X	X